University POLITEHNICA of Bucharest
Faculty of Power Engineering
Energy Doctoral School

PHD THESIS SUMMARY

RESEARCH ON STRUCTURAL MATERIAL EMBRITTLEMENT MECHANISMS IN LIQUID LEAD ENVIRONMENT FOR GENERATION IV NUCLEAR REACTORS

PhD supervisor:
Prof. Dr. Eng. Ilie PRISECARU

PhD student:
Livia-Nicoleta SAFTA (STOICA)

Scientific consultant:
PhD Physics Vasile RADU

BUCHAREST
2022

University POLITEHNICA of Bucharest
Faculty of Power Engineering
Energy Doctoral School

RESEARCH ON STRUCTURAL MATERIAL EMBRITTLEMENT MECHANISMS IN LIQUID LEAD ENVIRONMENT FOR GENERATION IV NUCLEAR REACTORS

PhD student:

Livia-Nicoleta SAFTA (STOICA)

DOCTORAL COMMITTEE

Professor Cristian DINCA University Politehnica of Bucharest	Chairman
Professor Ilie Constantin PRISECARU University Politehnica of Bucharest	Supervisor
Professor Daniel DUPLEAC University Politehnica of Bucharest	Reviewer
Professor Serban Constantin VALECA Institute for Nuclear Research Pitesti	Reviewer
Professor Marian Cătălin DUCU University of Pitesti	Reviewer

BUCHAREST
2022

Foreword,

„We should never lose two virtues: the courage to face our weaknesses and the strength to experience our own emotions."

(Michelangelo Buonarroti)

Now, at the end of a fruitful and important period for me, I feel deeply overwhelmed by wonderful feelings and happiness and I would like to say a few words of thanks to those who guided or supported me during this doctoral study.

I express my gratitude to the Management of the ***Institute for Nuclear Research Pitesti****, which provided the necessary support for the doctoral thesis.*

I would like to express my special thanks to Dr. Fiz. CS II ***Vasile RADU****, for his scientific altruism and exemplary pedagogy, has proven to share the richness of theoretical and experimental information in the field of materials engineering, for the suggestions, observations and discussions he offered me throughout the preparation of my doctoral thesis. I am deeply grateful for the effort and advice gave during the development of this scientific approach.*

Special thanks to Professor Dr. Eng. ***Ilie PRISECARU****, for the permanent guidance and support of all the teachers from the Department of Energy Doctoral School of UPB, who participated in the evaluation of my studies and allowed me to prepare my doctoral thesis and write it in a proper form.*

I would like to thank all the wonderful colleagues from Section III, the "Thermomechanical and Microstructural Properties" Collective, with whom I collaborated and who guided me during the elaboration of this important professional study. In particular, I would like to thank my colleagues for their support in carrying out the experimental part of the thesis: Dr. CS III ***Alexandru NITU****, Dr. CS III* ***Viorel IONESCU****, Op.* ***Marius CONSTANTINESCU****.*

With special love and affection, I thank my husband, ***Marius****, who was with me and who supported me with his affection and patience throughout this complex period of my professional life.*

I want to dedicate this thesis to my child, ***Octavian****, who I hope will understand the essence of the following proverb: "The roots of learning are bitter, but its fruits are sweet, and a book is like a gold bar."*

Thank you!

Drd. Livia-Nicoleta STOICA

CONTENTS OF THE DOCTORAL THESIS

List of works

ISI listed journal articles:

1. **Livia Stoica**, Vasile Radu, Alexandru Nitu, Ilie Prisecaru, „Development of a model for the crack initiation and growth simulation of the structural materials under liquid metal embrittlement conditions", *Journal of Science and Arts, No.3 (56), pp. 831-844, 2021, Physics Section, ISSN: 1844-958.* ***Note: Contains partial results from the research of the doctoral thesis.***
2. **L.-N. Stoica,** V. Radu, Al. Nitu, I. Prisecaru, „Study of the Structural Mechanical Behavior in Liquid Lead Environment for the ALFRED Generation IV Reactor*", 2021, 10th International Conference on ENERGY and ENVIRONMENT (ICES), 2021, PP1-4, DOI: 10.1109 / CIEM52821.2021.9614891;* ***Note: Contains partial results from the research of the doctoral thesis.***
3. **Livia Stoica,** Alexandru Nitu, Vasile Radu, „Study on the Mechanical Properties of Generation IV Innovative Materials by Non-standardized Method, *Romanian Journal of Physics, Volume 65, Number 5-6, 904 (2020)*.
4. Alexandru Nitu, **Livia Stoica,** Vasile Radu, „Development of the fracture toughness methodology for the small tubes used in the generation IV reactors", *UPB Sci. Bull., Series B, Vol. 82, Iss. 1, 2020 ISSN 1454-2331.*

Articles in national / international journals / conferences:

5. **Livia STOICA**, Vasile RADU, Alexandru NITU, Viorel IONESCU, Denisa TOMA, „A new approach to obtain Ramberg-Osgood constitutive equation for materials used in structural components of nuclear reactors"**,** *Journal of Nuclear Research and Development, 2021, ISSN 2247-191X ISSN-L 2247-191X, No.20, May.*
6. **Livia STOICA,** Vasile RADU, Alexandru NIȚU, Denisa TOMA, Valentin OLARU, „A Critical Review of the Liquid Metal Embrittlement Models as Support for Generation IV Materials Damage Analysis", *The 13the Annual International Conference on Sustainable Development through Nuclear Research and Education, 26-28 May 2021 Pitesti, Romania.*
7. V. Olaru, E. Matei, A. Nitu, L**.N. Stoica**, D. Toma, M. Matei, „Mechanical fatigue tests of SEU-43 fuel bundle cladding at 400 °C", *EMERG 2021 ISSN 2668-7003 ISSN-L 2457-5011 - Vol 7, Issue 1, pp. 151-158 (2021), DOI: 10.37410 / EMERG.2021.1.12.*
8. Vasile RADU, **Livia STOICA**, Denisa TOMA, Valentin OLARU, „Study on the Integration of the Creep Law from Artificial Neural Network Methodology in the Delayed Hydride Cracking Assessment of the CANDU Pressure Tubes", *Journal of Nuclear Research and Development, No.22, December 2021.*
9. V. Ionescu, V. Cojocaru, Al. Nitu, **L. Stoica**, V. Olaru, D. Toma, „Study To Set Up The Experimental Facility For The Ultrasonic Measurements In The Liquid Lead", *Journal of Nuclear Research and Development, No.22, December 2021.*
10. Vasile RADU, **Livia STOICA**, Alexandru NIȚU, Denisa TOMA, Valentin OLARU, „Study to assess the ductile fracture in Zr-2.5% Nb by J-integral with the Finite Element Method using the Gurson-Tvergaard-Needleman Model", *The 13 th Annual International Conference on Sustainable Development through Nuclear Research and Education, 26-28 May 2021 Pitesti, Romania.*
11. Viorel IONESCU, Virgil COJOCARU, Denisa TOMA, Alexandru NIȚU, **Livia STOICA**, Valentin OLARU, "Study to set up the experimental facility for the ultrasonic measurements in the liquid lead", *The 13 th Annual International Conference on Sustainable Development through Nuclear Research and Education, 26-28 May 2021 Pitesti, Romania.*
12. Alexandru NIȚU, Laurențiu AIOANEI, Andrei VÎLCU, Vasile RADU, Marian HOROROI, Viorel IONESCU, **Livia STOICA**, Denisa TOMA, Valentin OLARU, „Control System Development for Liquid Lead Testing Installation", *The 13 th Annual International Conference on Sustainable Development through Nuclear Research and Education, 26-28 May 2021 Pitesti, Romania.*
13. Denisa TOMA, Alexandru NIȚU, Laurențiu AIOANEI, Andrei VÎLCU, **Livia STOICA**, Alexandru Florea, Valentin OLARU, Ionescu VIOREL, „Study on the Development, Implementation and Analysis of Software Programs for the Acquisition and Control of Working Parameters for the Experimental Test Facility in Liquid Lead Environment ", *The 13 th Annual International Conference on Sustainable Development through Nuclear Research and Education, 26-28 May 2021 Pitesti, Romania.*
14. V. Radu, **L. Stoica** , V. Olaru, Al. Nitu, V. Ionescu, M. Mihalache, „Analysis of Creep-Induced Strains and Stresses in the V Notches Process Zone from the CANDU Pressure Tubes", *Journal of Nuclear Research and Development, No. 19, May 2020, ISSN 2247-191X , ISSN-L 2247-191X.*

15. V. Ionescu, V. Radu, Al.Nitu, **L. Stoica**, V. Olaru, M. Mihalache, D.Toma, „Study on Establishing the Cracking Criterion due to Mechanical Overload of the Zr-2.5% Nb Pressure Tube Specimens with Volumetric Flows " *, Journal of Nuclear Research and Development, No. 19, May 2020, ISSN 2247-191X, ISSN-L 2247-191X.*
16. **L. Stoica,** V. Radu, "Fatigue crack initiation at complex flaws in hydride Zr-2.5% Nb samples from CANDU pressure tubes", *The 9th Annual International Conference on Sustainable Development through Nuclear Research and Education 18-20 May 2016 Piteşti, Romania*.
17. **L. Stoica**, S. Valeca, Al. Nitu, „Failure analysis on CANDU structural materials by DHC mechanism", The 8th Annual International Conference on Sustainable Development through Nuclear Research and Education 27-29 May 2015 Piteşti, Romania.
18. **L. Stoica**, S. Valeca, Al. Nitu, „Study of the mechanical properties of Zircaloy-4 alloy by the *ring tensile test* method ", *Scientific Conference on Research and Development with international participation "Knowledge for the development of renewable energy systems", Pitesti, March 27-28, 2015.*

Abstract

In the doctoral study, the experimental mechanical tests were performed on 316L steel, in a systematic approach, in the liquid lead and the air environments at temperatures of interest for the ALFRED (Advanced Lead Fast Reactor Demonstrator), which will be built up at RATEN ICN, Romania. The result is a complex matrix of experimental data for the analysis of the Liquid Metal Embrittlement (LME) phenomenon. At the same time, a complex analysis of the experimental matrices was performed: numerical analyzes with MATLAB, microstructural and SEM analyses. The elastoplastic behavior of a ductile material under uniaxial stress in tensile tests in the air and liquid lead environments was characterized by constitutive equations of Ramberg-Osgood type. A new method for obtaining the coefficients defining the Ramberg - Osgood constitutive equation has been proposed. An original aspect of the doctoral study on the effect of LME is the use of the Multilayer Feedforward Neural Network method, in the processing of experimental data. Thus, there are obtained the prediction functions for the parameters of the Ramberg - Osgood equation, having as input variables: test temperature, deformation speed, yield stress, ultimate tensile strength. Within the own contributions of the doctoral study is presented a complex application of practical use of the results for structural integrity. This consists of implementing a model to evaluate the initiation and propagation of cracks under LME conditions on 316L austenitic stainless steel, using the finite element method in the specialized fracture mechanics software. The results of the doctoral study will be used practically in the structural integrity analysis activities, performed with some computer codes for the assessments of the ALFRED demonstrator.

***Keywords*:** liquid lead embrittlement, tensile test, microstructural analyses, constitutive equations, artificial neural network method, structural integrity.

1. INTRODUCTION

The availability of energy resources, climate change, and air quality and energy security plays an increasingly important role for nuclear energy in future energy sources. While current Generation II and III nuclear power plant projects provide economically acceptable electricity and public supply in many markets, further advances in the design of the nuclear power system may expand the opportunities for the use of nuclear energy. To explore these opportunities, governments, industry, and research centres around the world have begun a comprehensive analysis of the possibilities for developing next-generation nuclear power systems, known as "Generation IV" [1].

"Generation IV" nuclear power comes with a precise and practical answer to the demand for clean and safe nuclear energy. The demands of modern society, expressed as the parameters of sustainable development, are fully met by these new energy systems. In Generation IV nuclear reactors, the European option is to develop liquid metal (sodium or lead) or gas-cooled systems. Romania's efforts in the field are integrated into joint research with prestigious research centres and partners in Italy, Germany, Belgium, Spain, Sweden and the Czech Republic. Technological competition is fierce, and the EU's fourth-generation R&D activity is fiercely competitive in Russia and the United States [2].

The “liquid metal embrittlement” phenomenon, that can occur in some Generation IV reactor configurations is a complex phenomenon that strongly depends on the specific solid-liquid torque. This phenomenon can lead to the embrittlement of some metals, which are ductile in the air and can become brittle in long contact with certain liquid metals. Many theoretical and experimental studies in the literature are dedicated to Liquid Metal Embrittlement (LME) to understand the basic mechanisms and develop the most reliable models to avoid the LME phenomenon in Generator IV reactor projects.

Romania, through RATEN ICN Pitești, is involved in the construction of the ALFRED demonstrator (Advanced Lead Fast Reactor European Demonstrator), which is based on liquid lead cooling, which is also the motivation of this paper to focus on the issue of embrittlement structural materials specific to this type of the reactor.

Following the above, the objectives of the doctoral study are the following:

- Presentation of the problem of using liquid lead used as a cooling agent in generation IV reactors;
- Critical analysis of the models elaborated in the literature regarding the mechanisms of embrittlement with liquid metals;
- Carrying out experimental comparative tensile tests, in the air and liquid lead environment, on samples made of 316L steel, to highlight the LME mechanism determined by liquid lead;
- Realization of an atlas of metallographic and SEM analyzes, on the samples resulting from the experimental tests, for highlighting the fracture characteristics induced by the LME embrittlement of lead on 316L steel;
- Development of a new method for obtaining the parameters of the equation constituting mechanical stress - deformation, as Ramberg - Osgood type, to use them in structural integrity analyzes;
- Development of a parametric model, based on artificial neural network, type "Multilayer Feedforward Multilayer Neuronal Network", to obtain analytical equations of the parameters of the Ramberg - Osgood equation, which should include as input the following parameters: temperature, strain rate, yield limit, ultimate tensile strength. The model has practical utility in the analysis of the structural integrity of the various components of the ALFRED reactor;
- Development of an application of one's research using the Ramberg - Osgood equation with parameters obtained in the paper for an analysis of fracture mechanics. This analysis envisages the initiation and propagation of a crack in 316L austenitic steel in the liquid lead environment. The analysis is performed with specialized fracture mechanics software, FEACrack, which uses the finite element method to analyze the mechanical stress field in the material, and the process of crack initiation and propagation is based on the Gurson-Tvergaard-Needleman (GTN) model.
- Intercomparing the results of the doctoral study with similar data available from the literature.

The doctoral thesis **is structured** in seven chapters, organized according to the Experiments - Analyses - Modelling - Applications model. The following is a brief description of the objectives of each chapter.

The first chapter introduces the subject of the thesis, the scientific context in which the scientific approach of the paper takes place, and the motivation of the doctoral study.

Chapter II deals with the issue of the compatibility of structural materials with liquid lead in Generation IV reactors, targeting the ALFRED demonstrator that will be built at RATEN ICN Pitesti. The most important failure mechanism that can occur in liquid lead-cooled reactors is considered, namely the induced embrittlement of the LME type at the contact of liquid metal-solid metal.

The content of **Chapter III** envisages a detailed presentation of the main models proposed in the literature on the triggering of the LME mechanism at the contact between various liquid metals with solid metals, most of which are micromechanical models. At the same time, this chapter makes a critical assessment of these models, emphasizing their benefits and limitations. The chapter also presents the expected directions of our research.

Chapter IV contains a description of the experimental facilities developed for conducting experiments and analyzes on tensile testing of 316L steel in air and liquid lead. Also, mentioned are methods and recommendations for testing in the liquid lead, for sample preparation, testing conditions. The two installations, Walter + Bai (for air testing) and Instron (on which liquid lead testing facilities have been developed), are presented highlighting the test specifications (deformation speed, temperature, etc.).

Chapter V evaluates and interprets the results obtained. The experimental curves of mechanical stress - deformation in air and liquid lead, metallographic analyzes by optical microscopy and SEM analyzes of fracture surfaces are considered. The ductile-brittle characteristics appear, as well as the correlation of the analysis of the results obtained with the similar ones from the specialized literature are highlighted.

Chapter VI contains the original part of the research in the doctoral study, dedicated to the parametric evaluation of the fragility phenomenon in the liquid lead environment of 316L steel. Thus, a new method for obtaining the parameters of the Ramberg - Osgood constitutive equation is proposed, which reproduces the mechanical stress-strain behaviour in the elastoplastic field under the tensile stress deformation. At the same time, an original method of processing the experimental data obtained in the test matrices is proposed, by processing with the method of artificial neural networks, to obtain analytical equations for the dependence of the parameters of the Ramberg - Osgood equation depending on the test conditions. At the end of the chapter, an application of fracture mechanics is presented, regarding the LME-type embrittlement of 316L liquid lead steel, using a micromechanical model (Gurson - Tvergaard - Needleman) and the finite element method with FEACrack software.

Chapter VII is dedicated to the conclusions of the doctoral study.

The results of the doctoral study will be used practically in the structural integrity analysis activities, performed with the help of various calculation codes, which will be used in the evaluations of the ALFRED demonstrator, which will be built at RATEN ICN Pitesti, Romania.

2. PROBLEMS OF COMPATIBILITY OF STRUCTURAL MATERIALS WITH LIQUID LEAD IN GENERATION IV REACTORS

The use of heavy liquid metals, especially lead or liquid lead alloys (primarily LBE - Lead Bismuth Eutectic), in the concept of Generation IV Rapid Reactor (LFR) requires an assessment of their compatibility with structural materials, having considering the fast neutron spectrum. Although Western countries have experienced rapid sodium-cooled reactors, the expertise on the compatibility of stainless steels with sodium is not transferable to lead and its alloys, due to significant differences in their physical and metallurgical properties.

Liquid lead or lead alloy is corrosive to structural materials. The main parameters impacting the corrosion rate of steels are the *nature of the steel (material part), the temperature, the flow rate of the liquid metal and the concentration of dissolved oxygen in liquid lead.* One measure that can be taken to reduce the loss of elements in the steel alloy (usually nickel, which is a component of austenitic stainless steel and dissolved in the liquid lead) is to maintain a controlled amount of dissolved oxygen in the melt. Dissolved oxygen forms a layer of metal oxide on the steel surfaces in contact with the lead which protects the steel from dissolution and refreshes the metal oxide layer in case of erosion by the flowing heavy metal.

The experience gained with liquid metal cooled reactors in industrialized countries, namely the expertise on the compatibility of stainless steels with sodium, cannot be transferred to lead and its alloys, due to the significant differences in their physical and metallurgical properties [3].

The phenomenon of *embrittlement due to the liquid metal* (LME - Liquid Metal Embrittlement) consists in reducing the ductility and the resistance of a metal alloy, which is normally ductility when it is subjected to mechanical stress while it is in contact with the liquid metal which has the property of "wetting" the alloy.

Damage by LME can occur in a structural component from a crack already present if the component is already wet with liquid metal. This crack will later grow through the rest of the material until it breaks. In the scientific literature, it is mentioned that in real materials there are situations in which some microcracks remain stable even in contact with liquid metal (Pb), while other cracks become unstable and will develop under the influence of brittleness atoms that will fill the crack until at the top of it. As premises, to produce and ascertain the effect of LME, the following aspects are mentioned in the literature:

- Direct contact at the atomic scale of the solid phase and the phase of the brittle liquid metal (interpreted physically as "wetting");
- The application of sufficient mechanical stress, which although at the macroscopic scale is below the flow limit, at the microscopic scale at the level of the crack/defect will produce plastic deformations;
- The existence of mechanical stress concentrators or the pre-existence of obstacles to the movement of dislocations.

It should be noted that there is still no consensus on the methods to be used in terms of the basics for understanding the main mechanisms or engineering applications. Thus, liquid metal embrittlement is a complex phenomenon that requires an interdisciplinary approach, described below.

- <u>Physico-chemical processes for the interaction between liquid / solid and the transport of brittle atoms</u>.Mass transport and the interaction of fragile atoms are, in most cases, controlled by the rate at which cracks propagate. The two main mechanisms are the adsorption of liquid atoms at mechanical stress concentrators, the dissolution and condensation of solid atoms. "Adsorption of liquid atoms at the tip of the crack" is generally more accepted than "dissolution/diffusion / re-precipitation of solid atoms" and has been more successful in predicting the LME mechanism. The priority is a better understanding and consensus of these processes.
- Changes in the mechanical and physical properties of the solid metal were induced by the liquid / solid interaction. This can be, for example, a change in the cohesive force or the shear force. Some models do not specifically address this.
- Crack formation and propagation. The models analyzed in the doctoral study mainly address this. Of the LME models analyzed, only the GBEPM (Grain Boundary Embrittlement and Penetration Models) model addresses crack initiation and could be used as a starting point, provided the cracks are intergranular.

Embrittlement with liquid metal is a particularly complex phenomenon that strongly depends on the specific solid/liquid torque and LME for a given solid/liquid couple can invoke several competing mechanisms.

Factors influencing the mechanism of embrittlement with liquid metal (liquid lead) are the *chemical composition of solid and liquid metal, the grain size of solid metal, working temperature, deformation rate, mechanical stress, pre-exposure conditions before testing, degree of wetting*.

Oxygen control technology has been successfully applied in the liquid lead and lead-bismuth cooling systems for corrosion of structural materials. The development of chemical control and monitoring of heavy liquid metals is one of the critical issues for nuclear systems that use lead alloys either as a washing target or as a coolant in terms of contamination control and corrosion.

Important factors affecting the corrosion of liquid metals include operational, metallurgical and technological factors [4].

3. CRITICAL ANALYSIS OF THE MODELS DEVELOPED IN THE SCIENTIFIC LITERATURE FOR THE DESCRIPTION OF THE FRAGILIZATION MECHANISM WITH LIQUID METALS

Among the promising models proposed in the literature, to take into account the nature of the LME phenomenon, we mention *the reduction in surface energy model, the adsorption model that induces the reduction of cohesion, the enhanced dislocation emission model, the enhanced work hardening model, the dissolution-condensation, localized plasticity pattern and grain boundary penetration pattern*. These LME models have been described according to the main ideas, advantages, limitations and controversies in Table 1.

Table 1. *Main features of existing models for LME [5]*

Model	The main features	Model support	Limitations
Reduction in Surface Energy (RSE)	- Thermodynamic approach based on the reduction of surface energy for breaking in liquid metallic environment - The defect is usually intergranular	- Experimental support - Can qualitatively consider the effects of many experimental observations, e.g. temperature, deformation rate and grain size	- Lack of surface energy data prevents quantification of fragility - Does not take into account the mechanisms of atomic degradation
Adsorption Induced Reduction in Cohesion (AICRM)	- Adsorption of liquid metal reduces the strength of cohesion on the atomic planes - Defect occurs by transgranular or intergranular cleavage	- Can qualitatively consider the effects of many experimental observations, e.g. temperature, deformation rate and grain size - Fractographic support	- Difficult to quantify - No more experimental observations can be explained
Enhanced Dislocation Emission (EDE)	- Adsorption of liquid metal atoms facilitates dislocation motion - Defect occurs by localized micro-ductile coalescence	- Experimental support - Strong fractographic support - Many similarities with other cracking phenomena promoted by the environment	- No math analysis - Based on complicated fractographic analyzes - Lack of independent support
Enhanced Work Hardening (EWH)	- Adsorption of liquid metal atoms facilitates dislocation motion - Activation of the dislocation movement results in hardening and eliminates plasticity - Cracking is intermittent	- Experimental support for discontinuous crack growth - Can qualitatively consider the effects of many experimental observations, e.g. temperature, deformation rate and grain size	- No math analysis - Lack of experimental support for improved hardening
Localized plasticity that favours LME (Hancock & Ives)	- Liquid metal diffuses along the grain boundary before the crack tip and reacts with the dislocation matrix to reduce the breaking stress	- Correctly predicts that LMIE rupture is accompanied by extensive plasticity - Mathematical analysis showed that rapid cracking of LME is possible under these conditions - Can qualitatively consider the effects of many experimental observations, e.g. temperature, deformation rate and grain size	- Cannot account for transgranular rupture or fracture of single crystals in LME - Lack of experimental support for the concept of diffusion of liquid metals before the tip of the crack
Dissolution-Condensation (DCM)	- Crack growth is done by the stress-assisted dissolution of solid metal into liquid metal at the tip of the crack	- Limited experimental support	- Lack of experimental support - Predicts the wrong dependence of LME on the composition of liquid metals
Grain Boundary Penetration (GBPM)	- Promoted stress diffusion of the liquid metal along the grain boundaries before the crack tip - The presence of the fragile before the crack tip increases the sliding difficulties and reduces the crack resistance	- Can qualitatively consider the effects of many experimental observations, e.g. temperature, deformation rate and grain size	- No math analysis - Lack of experimental support for the concept of diffusion of liquid metals before the tip of the crack - Cannot account for transgranular fracture or crystal breakage by LME

Because none of the models can fully simulate all the experimental observations, they cannot be complete, admitting improvements or updates. The diversity of the models and the predictions made by each model reflects the experimental results based on which the investigations were performed. In addition, many difficulties are encountered in experimental testing to highlight the effect of LME, which prevents the development of a unified model that can make predictions for all situations encountered in practical reality.

The high temperatures required to test the LME in some metal systems have led to the use of simple techniques, usually uniaxial tensile testing, in the LME study. This is especially true for industrially important systems where lead, zinc and tin embrittlement are common [5]. In these tests, it is not always possible to separate the processes of initiation and propagation of cracks. As a result, the mechanisms by which these processes are initiated have not yet been established. Applying the concepts of fracture mechanics to the LME study should allow a clearer distinction between crack initiation and propagation and therefore lead to a better understanding of the LME phenomenon.

Metallographic and fractographic examination of LME fracture surfaces may also be useful in interpreting embrittlement processes. However, the difficulties encountered in the preparation and analysis of these surfaces have prevented the understanding of micro-failure mechanisms. LME tearing surfaces are usually covered with a liquid metal film, which can mask important graphic details. Physical and chemical cleaning methods have not been particularly successful and can lead to distortion or removal of fine details. Reactions between the liquid metal and the base metal can also lead to the formation or corrosion of the intermetallic compound, which can completely change the fracture surfaces.

Finally, the LME is generally considered to be a surface phenomenon, and as such, a thorough knowledge of surface conditions is required to understand the LME process. Therefore, the stress state, geometry, composition and structure of the surface layers and the solid/liquid interface and the effects of liquid metal adsorption on them must be determined before the LME can be more clearly understood. In this regard, recent advances in surface science and the analytical techniques and equipment available for the study of these variables should allow for a more complete investigation of this phenomenon.

To take into account the LME phenomenon in the design and operation of nuclear power reactors, which use heavy liquid metals as coolant, a practical engineering approach is needed, which can be used in structural analysis on innovative Generation IV materials, with the help of calculation codes specific to this issue. In principle, for LME assessments, it is difficult to separate the mechanistic approach from the engineering one, as the LME effect is inherently coupled with the fragility transport and the fracture mechanism.

One of the approaches of LME is to perform comparative tests in the liquid metal environment concerning identical tests performed in air, to detect the effect of LME on material properties. Thereafter, the transferability between LMEs, for a standard test, to a component operating under Generation IV reactor-specific conditions must be considered.

From the tests planned in the paper, tensile tests at various strain rates, including low strain rate (Slow Strain Rate Testing (SSRT)), LME prediction will be made by studying the influence of liquid metal environment on the characteristics of mechanical stress-strain. This will be done with the physical-mathematical methods, described in the doctoral thesis.

4. DESCRIPTION OF EXPERIMENTAL FACILITIES DEVELOPED FOR THE STRUCTURAL MATERIAL TESTING PROGRAM FOR INTERACTION WITH LIQUID LEAD

In this chapter, the mechanical tests performed in the doctoral thesis, to characterize the effect of LME on 316L steel, were presented by comparative tensile tests performed in air and liquid lead. The complete results will be presented and analyzed in a separate chapter of the doctoral thesis.

It should be noted that the mechanical tensile tests were mechanical tests performed at the strain rates of the samples, which were close to the characteristics of the SSRT tests. This type of test, recommended by ASTM G 129-00 [6], offers the possibility to highlight the influence of LME mechanisms on the material properties resulting from the testing. The existing installations within RATEN ICN Pitesti, a group of Thermo-mechanical and Microstructural Properties collective, were used for this type of tests, to which substantial improvements were made to perform the mechanical tests in a liquid lead environment.

<u>INSTRON installation used to perform tests performed in a liquid lead environment</u>

The experimental installation with which the tensile tests were performed is an INSTRON Mechanical Testing Machine, for which additional facilities have been developed to allow testing in the liquid lead. It has a maximum mechanical load capacity of 25 kN, three extensometers with an active length of 10, 25 and 50 mm, respectively, and has a measurement accuracy of 0.5%.

With the help of the experimental facilities developed on the INSTRON machine, uniaxial tensile tests can be performed in a configuration based on a crucible containing in static conditions, liquid lead, with temperatures up to 450 ºC. Until the traction tests are performed for the present doctoral thesis, a system for monitoring dissolved oxygen in the liquid lead has not yet been implemented. The entire experimental configuration implemented for the liquid lead testing, together with the INSTRON traction machine, is shown in Figures 1, 2, 3, 4.

The main parts of the installation are: the heating system, the melted lead crucible and the sample fixing assembly, the machine pull rod, the Instron tensile test system.

Figure 1. *Experimental test installation in a liquid lead environment*

Figure 2. *Heating system*

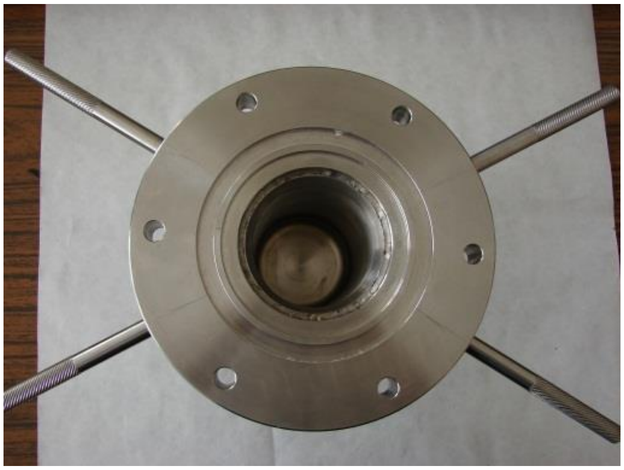

Figure 3. *Crucible for liquid lead*

Figure 4. *Clamping system for mechanical testing*

<u>WALTER + BAI installation used for tests in the air</u>

The installation with which the air tests were performed, at the temperatures of interest, is a Universal Mechanical, Servo-Hydraulic Testing Machine, Walter + Bai (figure 5). This machine can perform tests both at ambient temperature and in temperature conditions. To perform the tests in temperature conditions, the machine is equipped with an electric oven - maximum operating temperature 1200ºC - (figure 6) and a thermostatic chamber - maximum operating temperature 350ºC - (figure 7) that allows viewing the test online (in progress) and also allows the use of the video extensometer to record the distortion of the sample.

The mechanical load is measured with the force cell and the deformation using the extensometer, video-extensometer or LVDT (displacement transducer) on the piston of the mechanical test machine.

Figure 5. *Walter + Bai Universal Servo-Hydraulic Mechanical Testing Machine*

Figure 6. *Electric oven*

Figure 7. *Thermostatic chamber*

The Walter + Bai Mechanical Testing System for testing materials in static and dynamic mode has the following characteristics:

- Capacity ± 25kN in dynamic mode and 30kN in static mode;
- Types of tests - traction, compression, bending, axial fatigue, fracture mechanics;
- The type of drive - servo-hydraulic;
- Piston stroke 100mm or ± 50mm;
- Transducers - force (force cell), displacement (LVDT system on the piston), elongation (extensometer);
- Windows XP operating software;
- Windows $DION_{PRO}$ application software package.

The thermostatic chamber for the mechanics' tests (figure 7) has the following characteristics:

- The maximum temperature 350ºC, attached to the W + B Machine;
- Temperature controller to keep the test temperature constant.

Type of tensile test specimen

Flat samples of small size austenitic 316L stainless steel are used for mechanical testing (Figure 8).

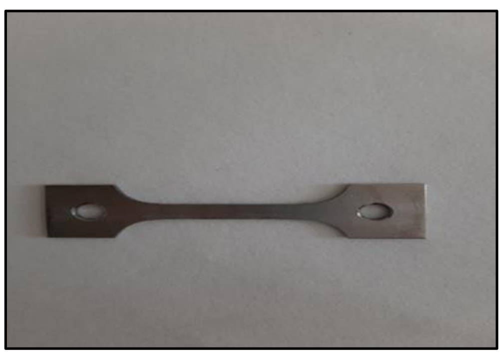

Figure 8. *316L sample used for mechanical testing*

5. EXAMINATION AND INTERPRETATION OF RESULTS OBTAINED IN EXPERIMENTAL TESTS PERFORMED IN THE AIR ENVIRONMENT AND THE LIQUID LEAD

This chapter covers microstructural analyses (optical microscopy and SEM) of samples subjected to tensile tests performed in the air and the liquid lead at three temperatures of interest and three rates of deformation, tests performed by the requirements of ASTM E8 [7] and ASTM G 129-00 [6].

At the end of the chapter is a comparative analysis of some results, obtained in the literature, on the embrittlement of 316L steel in eutectic bismuth lead (LBE), with significant results obtained in the doctoral thesis, which highlights the susceptibility to LME of mechanical behaviour for samples tested in the liquid lead.

The results of all tensile tests, according to the test matrix, will be processed in the form of Ramberg - Osgood type constitutive equations, which will be the original contribution of the doctoral thesis on the susceptibility of LME in the mechanical behaviour of 316L liquid lead steel.

The tables below (Table 2 and Table 3) show the test matrix in the air environment and the liquid lead environment, respectively, of the samples made of 316L austenitic steel and the parameters that define the Ramberg-Osgood equation. Ramberg – Osgood deformation equation [8] which will be used in the doctoral thesis, has the form used by the software for analyzing the parameters of fracture mechanics by the finite element method FEACrack [9]. Thus, the form of the Ramberg-Osgood equation on which the experimental data will be approximated/fitted is as follows:

$$\frac{\varepsilon}{\varepsilon_0} = \frac{\sigma}{\sigma_0} + \alpha \cdot \left(\frac{\sigma}{\sigma_0}\right)^{1/n} \qquad (1)$$

where:

σ_0 - is the reference voltage, which is usually given by the flow limit ($\sigma_{0.2}$);
ε_0 - reference deformation ($\varepsilon_0 = \sigma_0/E$, where E - Young modulus of elasticity), ($\varepsilon_{0.2}$);
n - hardening exponent;
α - material coefficient.

Table 2. *Air test matrix*

Temperature (°C)	Sample code	Low deformation speed (V1 -SSRT) $\dot{\varepsilon} = 5 \times 10^{-5} s^{-1}$	Sample code	Average strain rate (V2) $\dot{\varepsilon} = 1,6 \times 10^{-4} s^{-1}$	Sample code	High deformation speed (V3) $\dot{\varepsilon} = 1,6 \times 10^{-3} s^{-1}$
350 °C	PT36	$\sigma_{0.2}$, σ_u, n, α	PT33	$\sigma_{0.2}$, σ_u, n, α	PT30	$\sigma_{0.2}$, σ_u, n, α
375 °C	PT35		PT32		PT29	
400 °C	PT34		PT31		PT28	

Table 3. *Melted lead test matrix*

Temperature (°C)	Sample code	Low deformation speed (V1 - SSRT) $\dot{\varepsilon} = 5 \times 10^{-5} s^{-1}$	Sample code	Average strain rate (V2) $\dot{\varepsilon} = 1,6 \times 10^{-4} s^{-1}$	Sample code	High deformation speed (V3) $\dot{\varepsilon} = 1,6 \times 10^{-3} s^{-1}$
350 °C	PT7	$\sigma_{0.2}$, σ_u, n, α	PT4	$\sigma_{0.2}$, σ_u, n, α	PT1	$\sigma_{0.2}$, σ_u, n, α
	PT8		PT5		PT2	
	PT9		PT6		PT3	
375 °C	PT25	$\sigma_{0.2}$, σ_u, n, α	PT22	$\sigma_{0.2}$, σ_u, n, α	PT19	$\sigma_{0.2}$, σ_u, n, α
	PT26		PT23		PT20	
	PT27		PT24		PT21	
400 °C	PR 16	$\sigma_{0.2}$, σ_u, n, α	PT13	$\sigma_{0.2}$, σ_u, n, α	PT10	$\sigma_{0.2}$, σ_u, n, α
	PR17		PT14		PT11	
	PR18		PT15		PT12	

In the chapter on experimental data processing and modelling, the experimental curves will be employed by the defining mechanical parameters for the tensile test (as mentioned in the test matrices.). Also, the modelling will take into account the deformation rates, as well as the test temperatures of the experiments performed in the air. For the tensile tests performed in the liquid lead environment, the same type of test was used as in the air environment.

To evaluate the effect of LME on the tensile behaviour of 316L steel samples, some results obtained from the air and the liquid lead tests were reported.

To test the temperature of 350^{O}C and the rate of deformation $5 \times 10^{-5} s^{-1}$ (SSRT), in figure 9 are shown a comparison between the tensile behaviour of sample 316 in the air and liquid lead.

Figure 10 shows the mechanical stress-strain curves, obtained at the test temperature of 375 ºC, and a strain rate of $5 \times 10^{-5} s^{-1}$.

For the test temperature of 400 ºC, at the same deformation speed of $5 \times 10^{-5} s^{-1}$, in figure 11 are shown the engineering stress-strain curves, obtained in the air and the lead for the 316L samples.

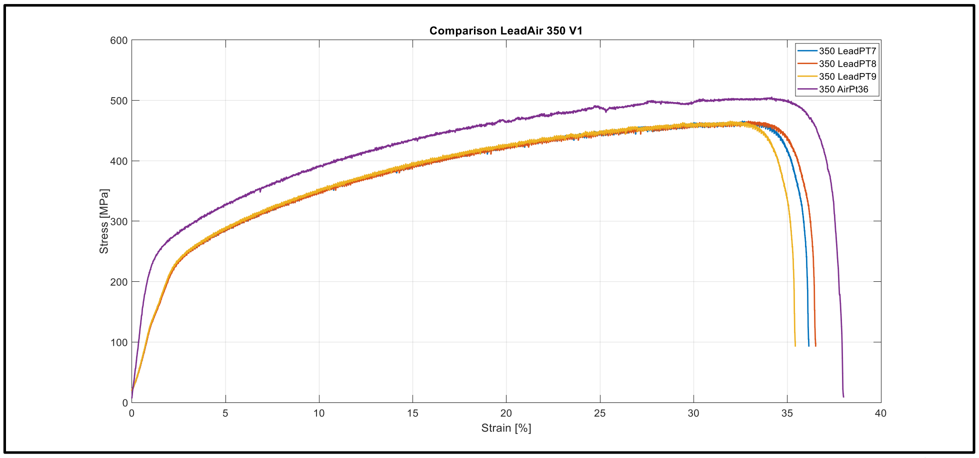

Figure 9. *Stress-strain curves in the air and lead, 350ºC, at a strain rate of* $5 \times 10^{-5} s^{-1}$

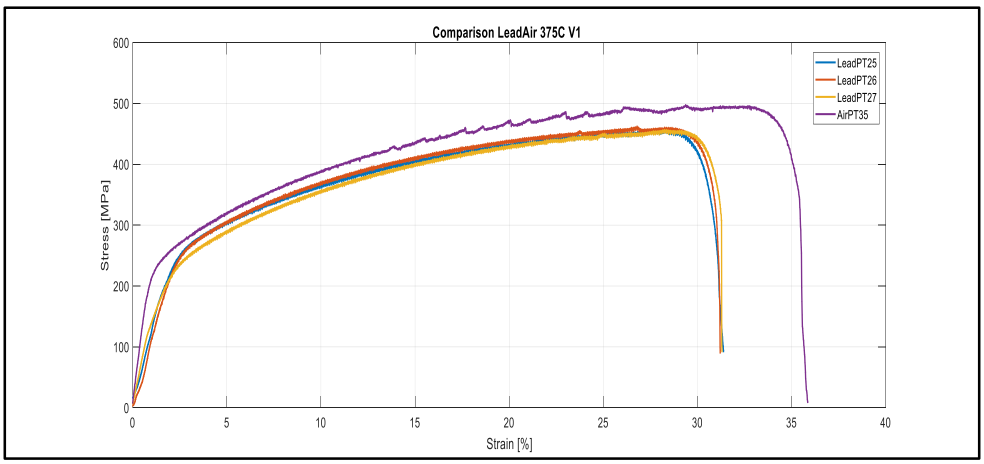

Figure 10. *Stress-strain curves in the air and lead, 375ºC, at a strain rate of* $5 \times 10^{-5} s^{-1}$

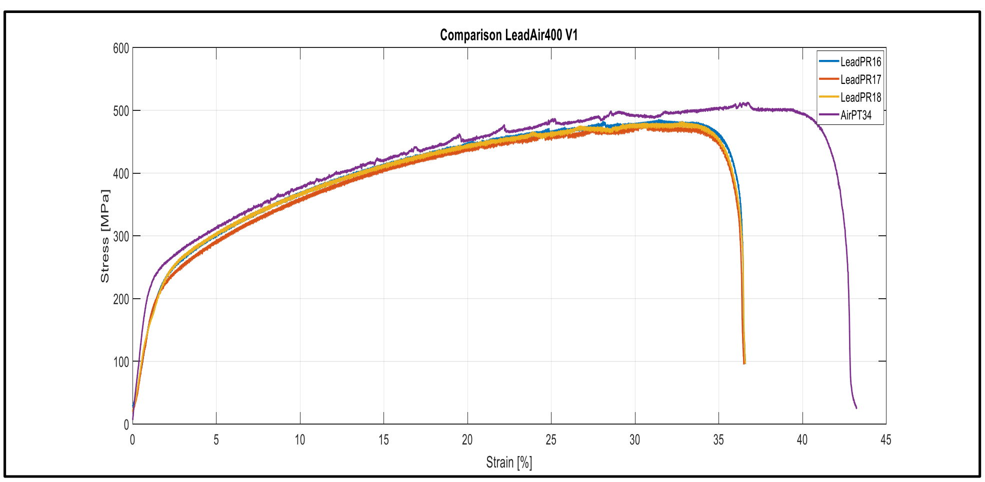

Figure 11. *Stress-strain curves in the air and lead, 400 ºC, at a strain rate of* $5 \times 10^{-5} s^{-1}$

Following the examination of the tensile curves mechanical stress-strain of the samples tested in air and liquid lead, the following statements can be made:

- It can be seen that for the temperature of 350 ºC, although the ultimate tensile strength decreases in the lead compared to the air, in terms of elongation at fracture, the difference is only a few percent.
- In contrast, for temperatures of 375 ºC and 400 ºC there is a decrease in ductility, by reducing the total deformation at fracture in the liquid lead environment compared to the tests performed in the air environment. This means that the presence of LME cannot be neglected at these strain rates in tensile. At the same time, there is a decrease in ultimate tensile strength for liquid lead testing, which can also be attributed to the LME effect on 316L samples, tested in SSRT. The full analysis of all tests performed at the specified temperatures and deformation rates will allow the detection of the LME effect as well as its modelling in the material constitutive equations.

It should also be noted that the performance of mechanical traction tests in liquid lead raises difficulties of analysis, due to uncertainties and possible errors in the acquisition of parameters of interest. This will be taken into account when processing the data to model the effect of LME on the behaviour of 316L liquid lead steel. Optical and electron microscopy (SEM) analyses will adequately complete the assumptions of LME aggression in the tests performed for the paper.

Optical microscopy analysis

The optical microscopy analyses were performed in the Mechanical Testing Laboratory, from RATEN ICN Pitesti, using a Zeiss Observer A1m microscope.

During the metallographic examinations with the help of the optical microscope, the microstructural aspect of the grain size was highlighted in the 316L steel samples (figure 12). It can be seen that the grain size varies in the range of 20-100μm. This is in line with the reference [10].

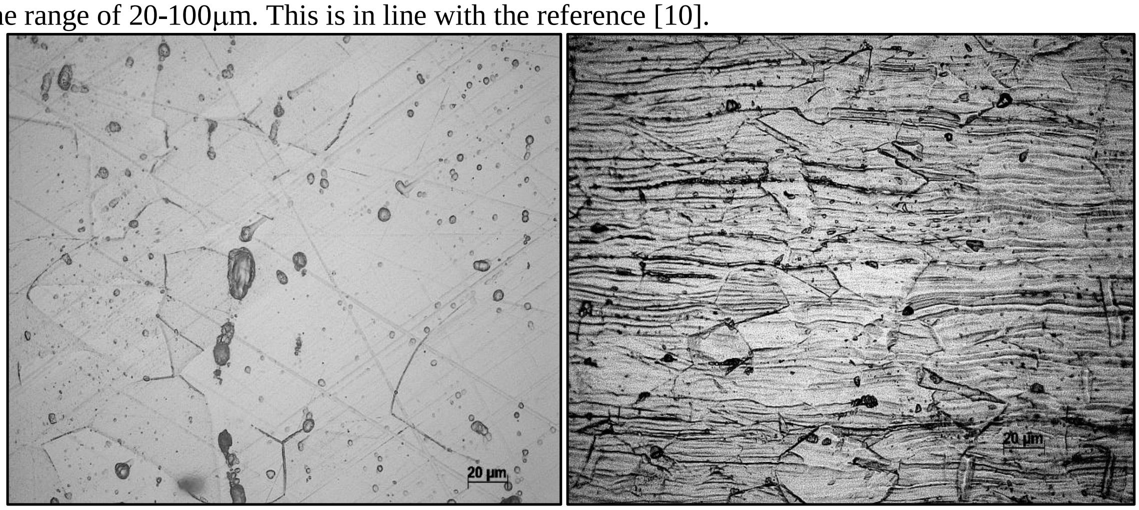

Figure 12. *The metallographic appearance of grain size on tested samples of 316L stainless steel*

The metallographic aspects of the fracture behaviour were analysed in the tensile tests performed in the air, respectively in the liquid lead, which confirms the propagation character of the cracking front. In principle, this can confirm the ductile, brittle or complex nature of the cross-section fracture of the samples.

Figure 13 (A), the front of the cracking breakage of the test sample in the air at 350ºC angles of 45º to the direction of mechanical loading, which characterizes a ductile behaviour. For samples tested at the same temperature in the liquid lead (Figure 13 (B)), the appearance of the crack propagation front is similar, which means that the presence of LME cannot be confirmed. This is in line with the elongation at fracture, shown in Figure 9, of the tensile curves.

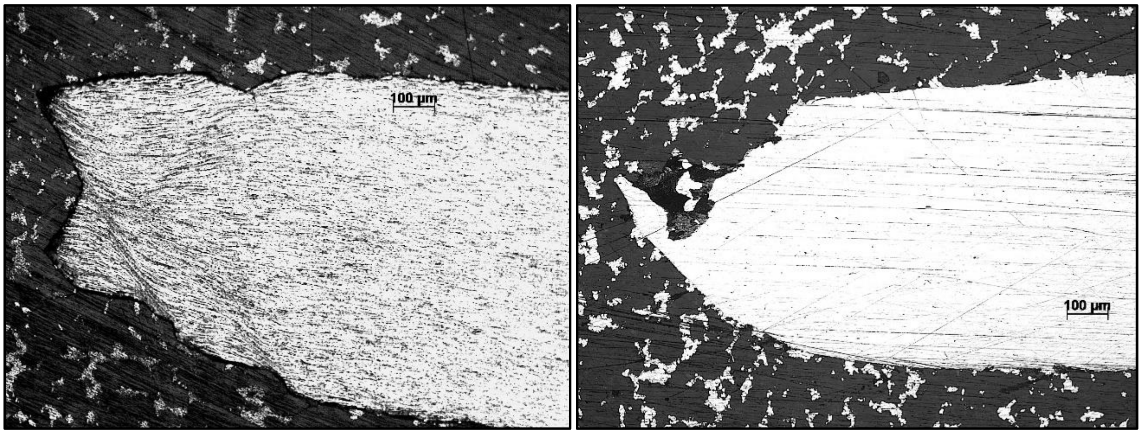

(A) 350ºC - Air (B) 350ºC - Lead

Figure 13. *Comparison of metallographic aspects of fracture fronts for air and lead samples tested at 350 °C*

At a temperature of 375ºC, samples were tested in the same air ductile behaviour, the above analysis, as can be seen from Figure 14 (A). In the case of lead-tested samples, at this temperature, the breaking edge begins to show a fragile appearance (Figure 14 (B)). This fragile aspect is represented by the segment of the crack propagation front which is perpendicular to the direction of mechanical stress. It should be noted, however, that in lead testing, the crack front has a mixed (ductile-brittle) character. It can be assumed that in the first part of the tensile test, the crack propagates ductile so that in the final part when the LME effect is felt by the sample by the penetration of lead into the incipient crack, the final rupture is of brittle type. The presence of the LME effect shown in Figure 14 (B) is consistent with the mechanical traction behaviour (Figure 10).

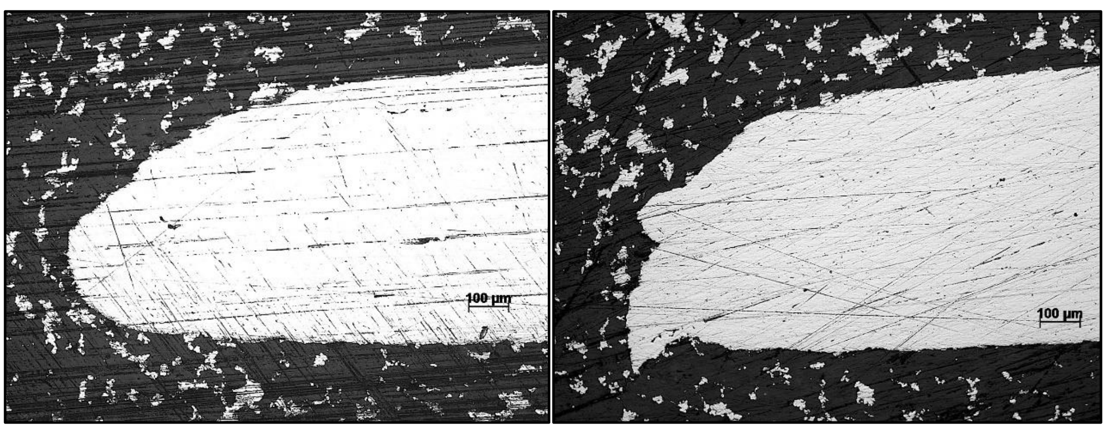

(A) 375ºC - Air (B) 375ºC - Lead

Figure 14. *Comparison of front cracking aspects of the metallographic samples tested in the air, and lead to 375 °C*

The above aspects are accentuated at the test temperature of 400 °C. Thus, in air testing the ductile appearance is even more pronounced, as can be seen in Figure 15 (A). For lead tests, the influence of LME on the rupture front is obvious, figure 15 (B), whose propagation is predominantly perpendicular to the direction of mechanical stress. Thus, the fragile type character of the fracture highlights the influence of the LME phenomenon both in the metallographic microstructural analysis and in that of the mechanical traction behaviour (figure 11).

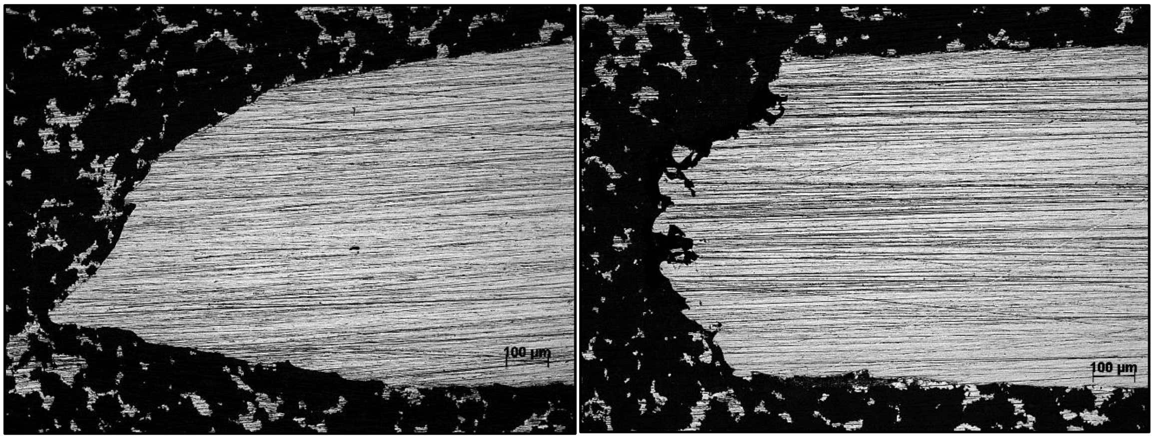

(A) 400^{o}C - Air (B) 400^{o}C - Lead

Figure 15. *Comparison of metallographic aspects of breakage fronts for air and lead tested samples at 400^{o}C*

Following the metallographic examinations of the samples tested in air and liquid lead, the following statements can be made:

- As can be seen from the examination of the tensile curves at 350 ºC, the behaviour of the samples, respectively of the cracking fronts, is not significantly different in lead from the air. The metallographic examination shows a ductile manner of propagation of the crack in the two test environments.
- For the temperatures of 375 ºC and 400 ºC a significant change of the character of the fracture front was observed, namely, the appearance of the features that characterize a brittle rupture. It can be assumed that this is due to the initiation of the LME mechanism during testing, especially at low strain rates (SSRT). This is in line with the observation of the decrease in ductility, by reducing the total deformation at fracture in the liquid lead environment compared to the tests performed in the air environment.

Scanning electron microscopy (SEM) analysis

For the SEM analyzes, within the doctoral thesis, the Tescan Vega LMU II scanning electron microscope was used, present in the Mechanical Testing Laboratory from RATEN ICN Pitesti.

From the SEM analyzes of the samples tested for the doctoral study, an atlas of representative images was prepared, organized for each sample as follows:

- An overview perpendicular to the fracture surface at a magnification of x150;
- And three depth images at x1000 magnification in three areas of the fracture surface.

In this way, we will have a complete and detailed picture of the fracture modes for the air and lead tested samples.

SEM analyzes for 350 ℃

The SEM analysis of the fracture surface of an air-tested sample is shown in Figure 16. For the lowest deformation velocity (SSRT type), the formation of microcavities (gaps) is noticeable in all three areas A, B, C, and some of them are placed inside larger cup-cone cavities. This way of cracking is typical of ductile fracture of metals.

For the tests performed in the liquid lead, for the lowest deformation rate (SSRT type), the SEM analyzes of the fracture surfaces (figure 17) show the same morphology of microcavities similar to the tests performed in air, namely, large cavities whose walls contain microcavities (goals). This is consistent with metallographic analysis by light microscopy at this temperature. Thus, it can be noted that the presence of LME due to lead is not highlighted by the SEM analyzes either.

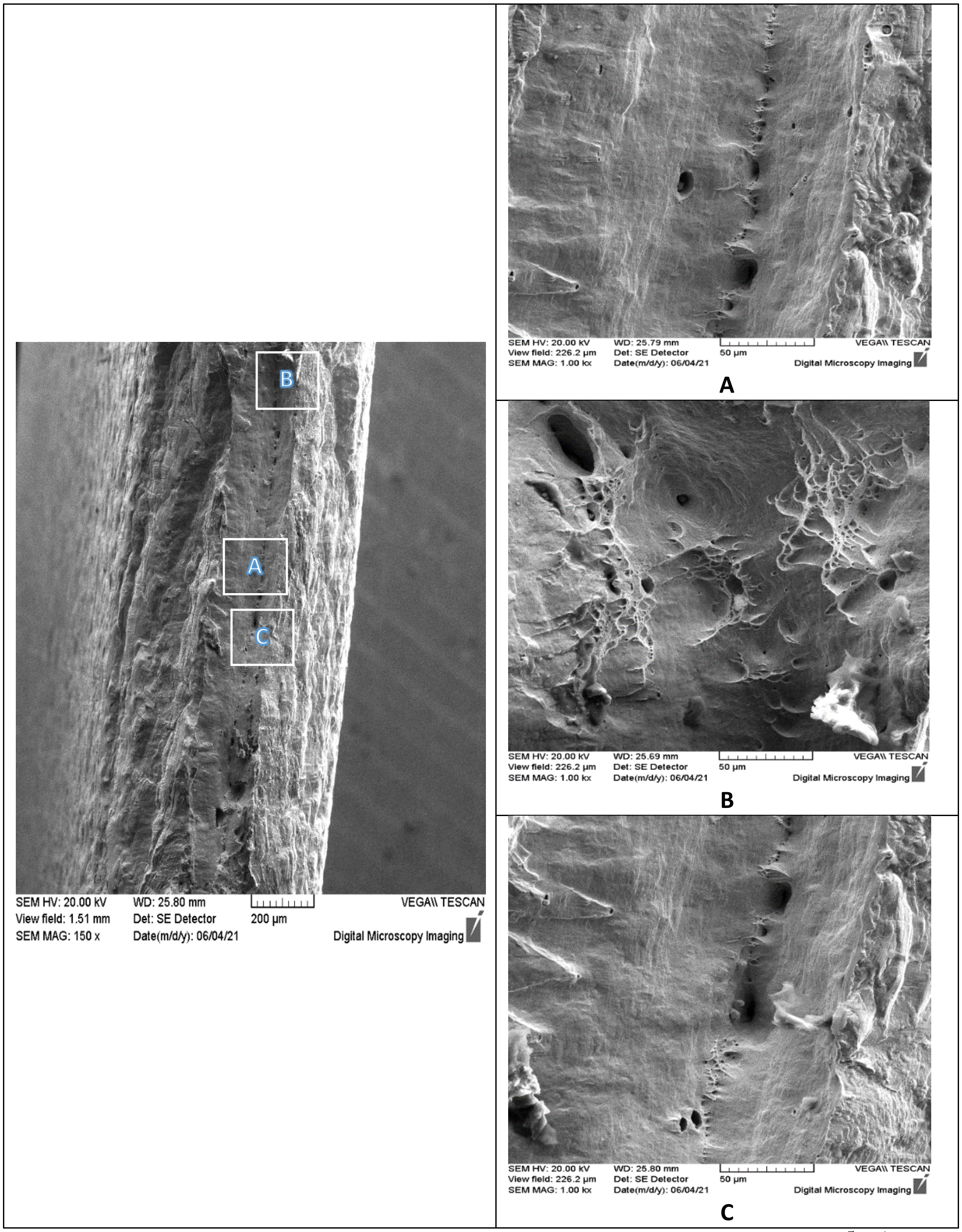

Figure 16. *SEM analysis of the sample PT36 tested in the air at 350ºC,* $\dot{\varepsilon} = 5 \times 10^{-5} s^{-1}$

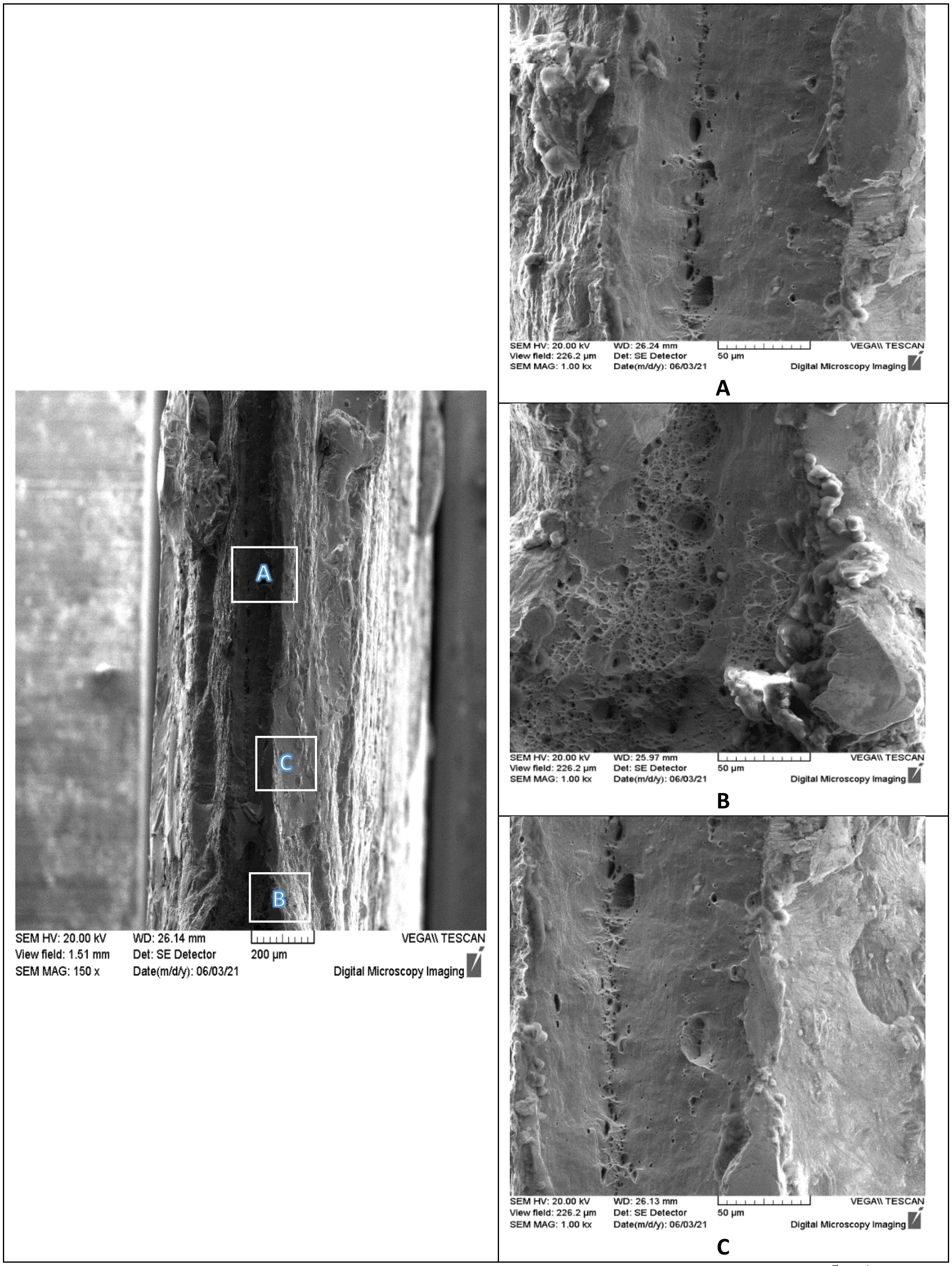

Figure 17. *SEM analysis of the sample PT7 tested in the lead at 350°C,* $\dot{\varepsilon} = 5 \times 10^{-5} s^{-1}$

SEM analysis temperature of 375°C

For tensile tests performed at the air at this temperature, a typical SEM surface is shown in Figure 18 for SSRT. And in this situation, for the three areas of the fracture surface observed at the increase of x1000, the morphology of the microcavities is similar to that observed at the temperature of 350°C. Thus, the ductile character of the specific fracture of metals is maintained.

For the tensile tests performed in the liquid lead at this temperature and strain rate (SSRT) (Figure 19), the mixed ductile-brittle character appears. Thus, a part of the fracture surface has microcavities (ductile rupture), it is bordered by an area with a micro-cleavage aspect (figure 31, C). This is certainly due to the LME mechanism caused by the liquid lead during the tensile test.

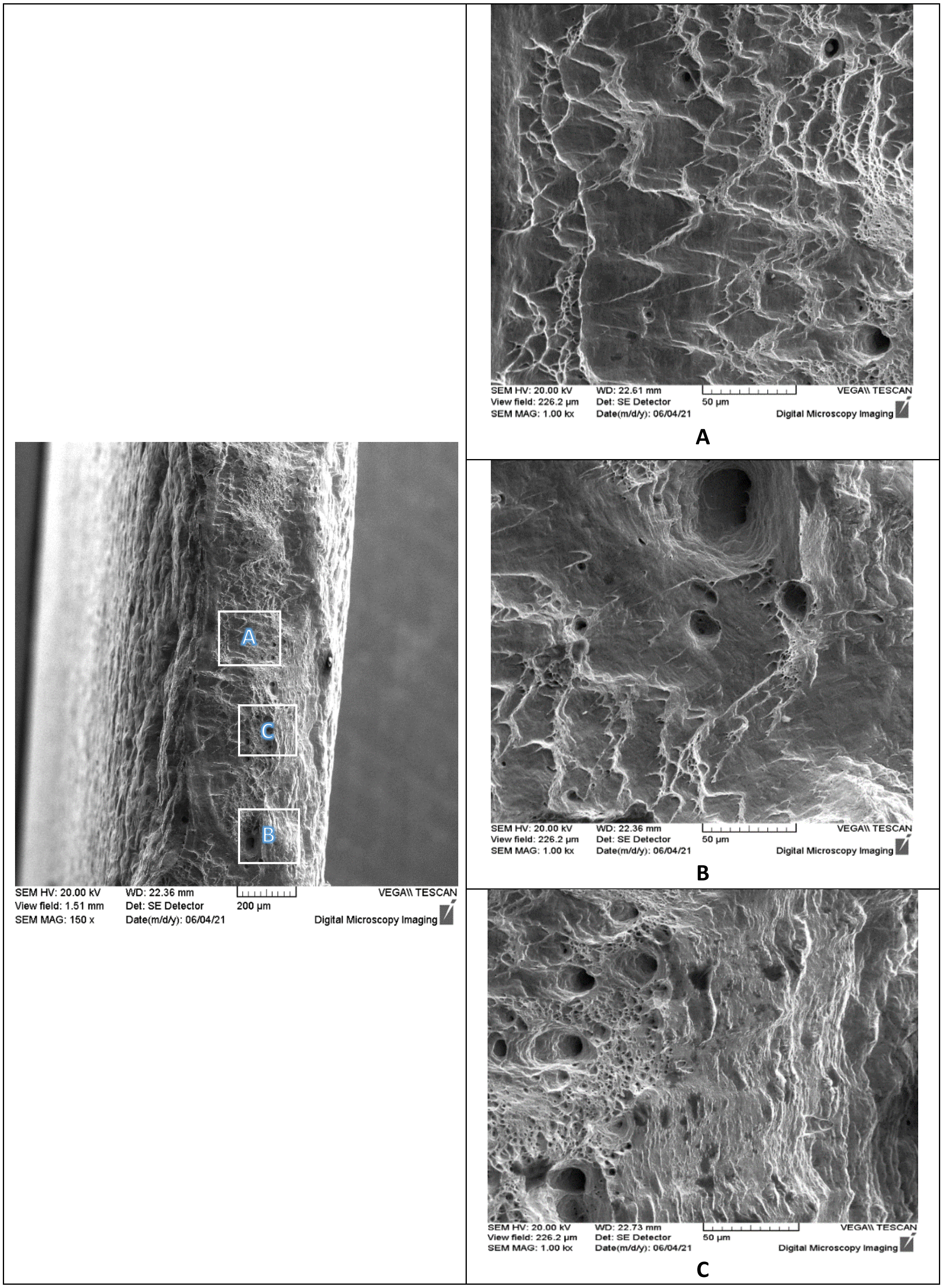

Figure 18. *SEM analysis of the sample PT35 tested in the air at 375 ℃,* $\dot{\varepsilon} = 5 \times 10^{-5} s^{-1}$

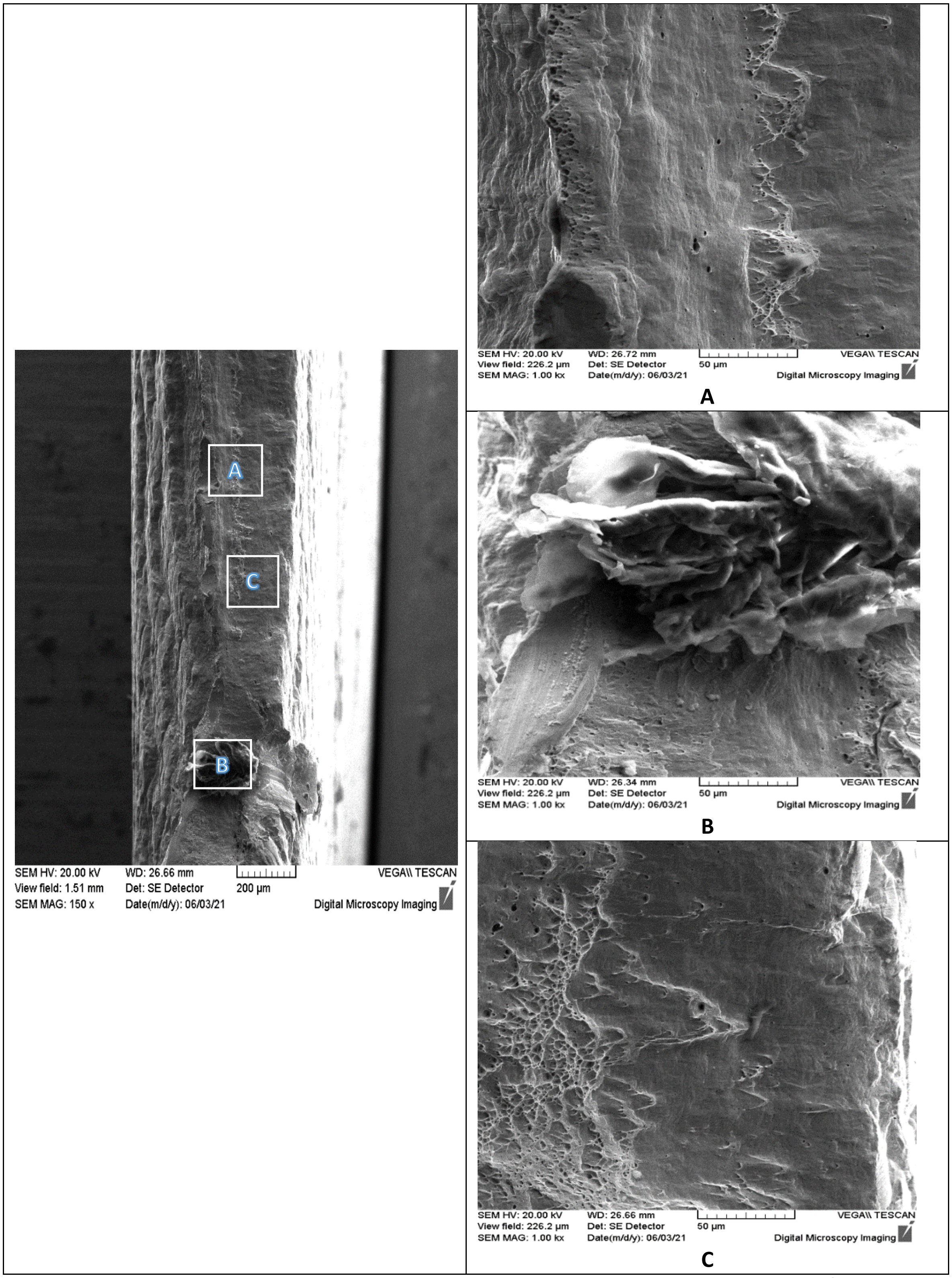

Figure 19. *SEM analysis of the sample PT25 tested in the lead at 375 ℃,* $\dot{\varepsilon} = 5 \times 10^{-5} s^{-1}$

SEM analyzes for 400℃

For tensile tests performed at the air at this temperature, a typical SEM surface is shown in Figure 20, for SSRT strain. In this situation, for the three rupture zones observed at the increase of x1000, the morphology of the microcavities is characterized by an increase in their dimensions as well as by the multiplication of the larger cavities. This can be explained by the increased ductility of 316L steel as the temperature increases.

For tensile tests performed in the liquid lead at this temperature and deformation rate (SSRT type) (Figure 21), the fracture surface mainly shows the cleavage areas confirming the fragility of the LME produced by liquid lead during the tensile test. The cleavage surfaces are quite large (figure 21, A, B, C).

SEM observations of fracture surfaces of samples tested in air and liquid lead at 400 °C are fully consistent with the metallographic observations.

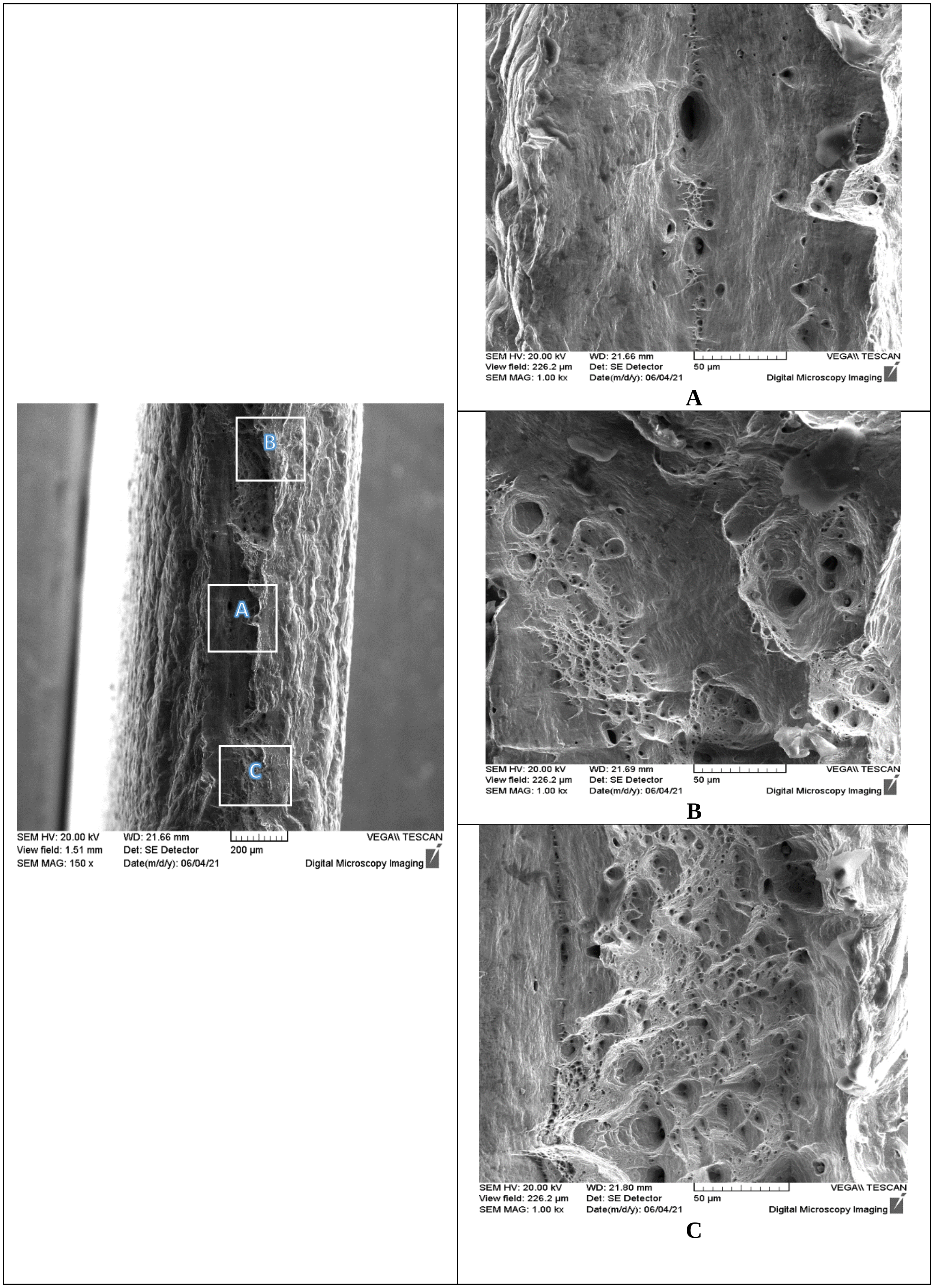

Figure 20. *SEM analysis of the sample PT34 tested in air at 400 ℃,* $\dot{\varepsilon} = 5 \times 10^{-5} s^{-1}$

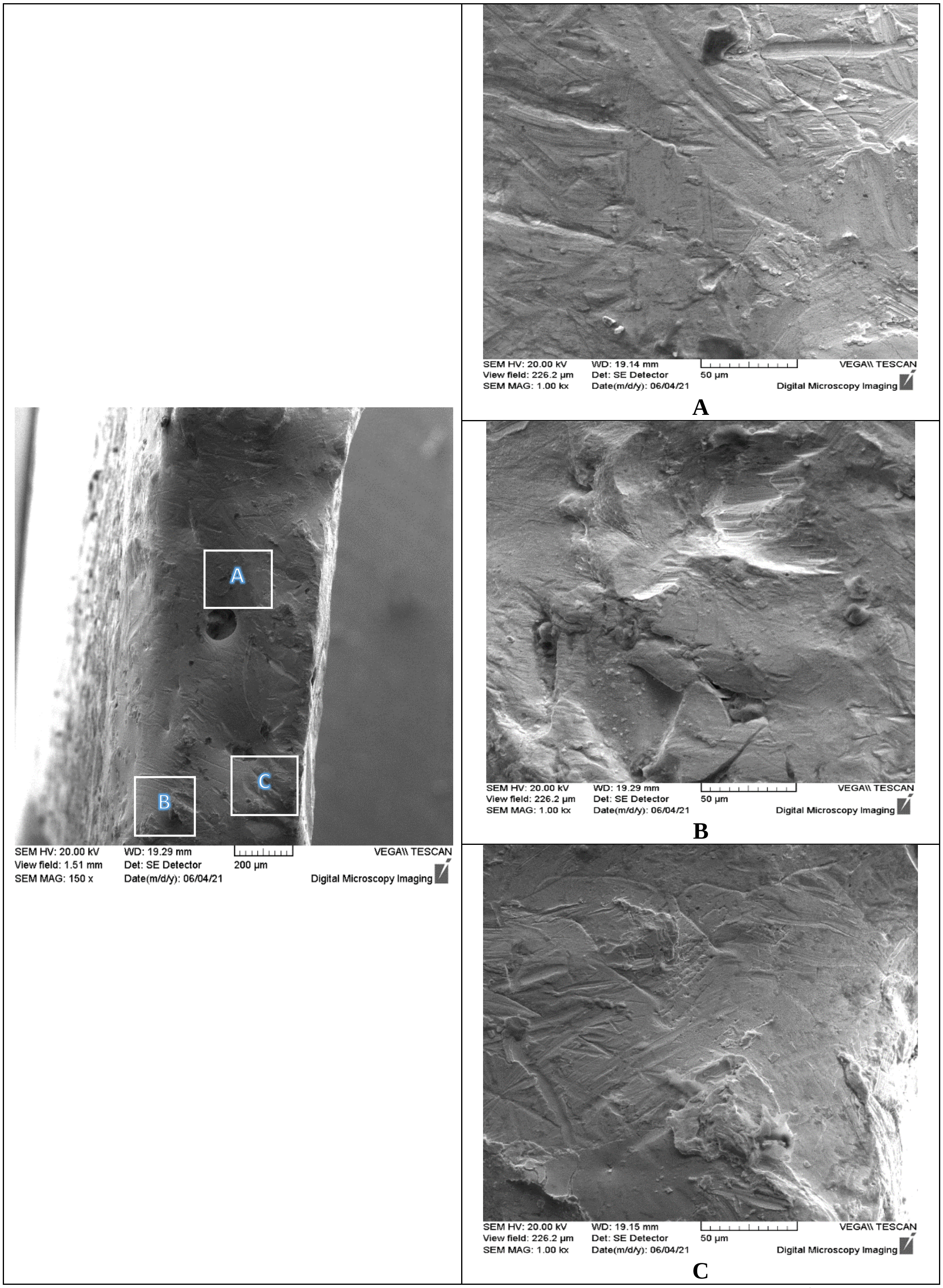

Figure 21. *SEM analysis of PR17 sample tested in the lead at 400 ℃,* $\dot{\varepsilon} = 5 \times 10^{-5} s^{-1}$

<u>Intercomparison of the results obtained with those in the literature on the susceptibility of LME to 316L</u>

Although few, the works mentioning the 316L in liquid lead confirm almost entirely the fragility effect induced by the liquid lead environment on the steel subjected to various mechanical tests: traction, small punch tests, mechanical fatigue, creep, breaking mechanics [11].

In Figure 22 (A), taken from the reference [12] is shown the force dependence as a function of transverse displacement for a sample of 316L in the inert environment and LBE. Although the test temperature is quite low (160 °C), there is a difference in the mechanical behaviour in the two environments. Figure 22 (B) shows the mechanical stress-strain curves, obtained for the doctoral study, at the request of the sample in the liquid lead at a temperature of 350°C. are significantly different and the higher influence of lead at 350°C.

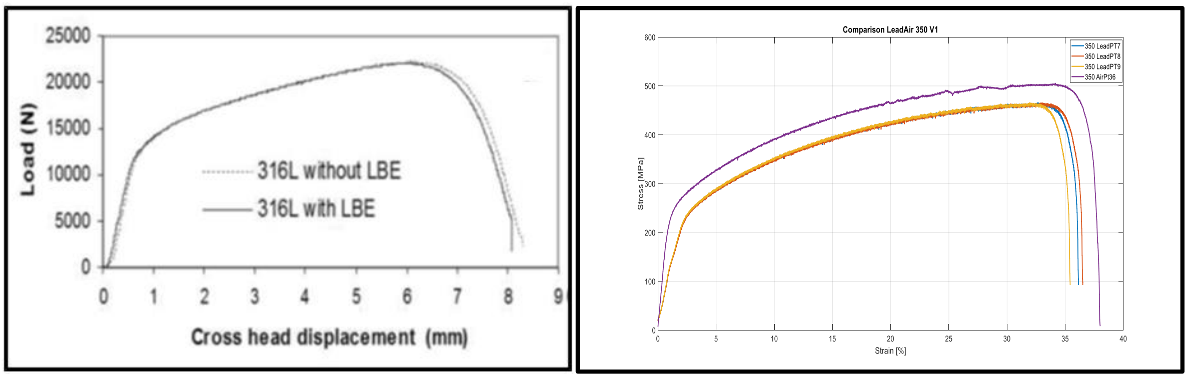

(A) *(B)*

Figure 22. *Tensile curves from (A) [12] 160°C in an inert environment and LBE, respectively (B) of this work*

In terms of metallography, the grain morphology of the 316L material tested in LBE [13] is similar to the grain morphology of the 316L samples tested in this paper. Thus, it can be seen that the grain size varies in the range of 25 - 100μm (figure 23).

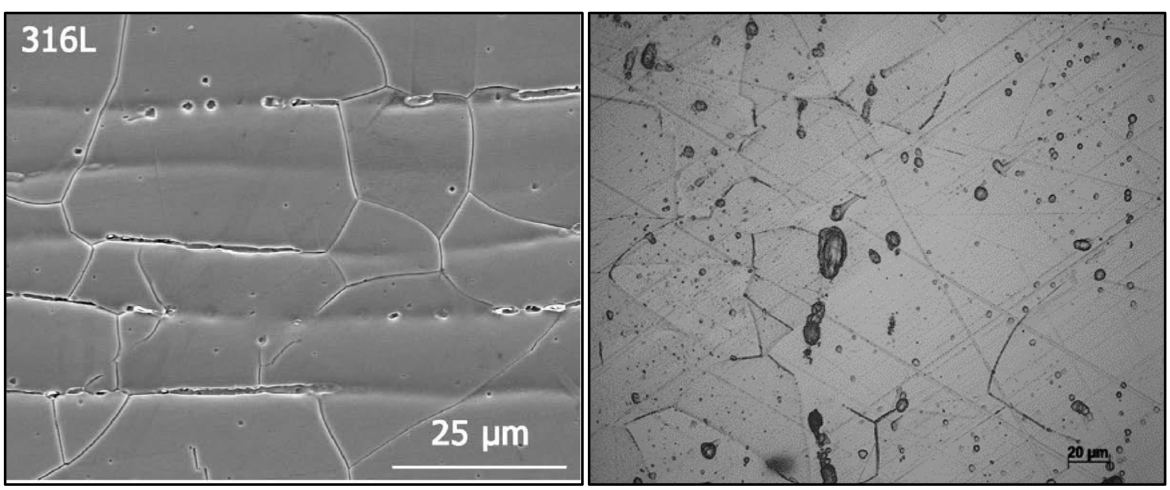

(A) (B)

Figure 23. *Grain morphology of 316L steel in (A) [13] and (B) - of this paper*

The effect of LME type is more pronounced in the SEM analyzes of the fracture surfaces for the samples tested in an inert or air environment, respectively in LBE or liquid lead environment. Thus, the reference [12] mentioned character ductile if the fracture surface in the inert environment samples of 316 tested at 160°C (Figure 24 (A)) or the mixed nature ductile-brittle of fracture surface in the LBE samples of 316 tested at 160°C (Figure

24 (B)). For the tests performed during the work at 375°C, in the air environment, the SEM morphology of the fracture surface has a ductile character, figure 24 (C), respectively mixed ductile-brittle character for the sample tested in the liquid lead (figure 24 (D)).

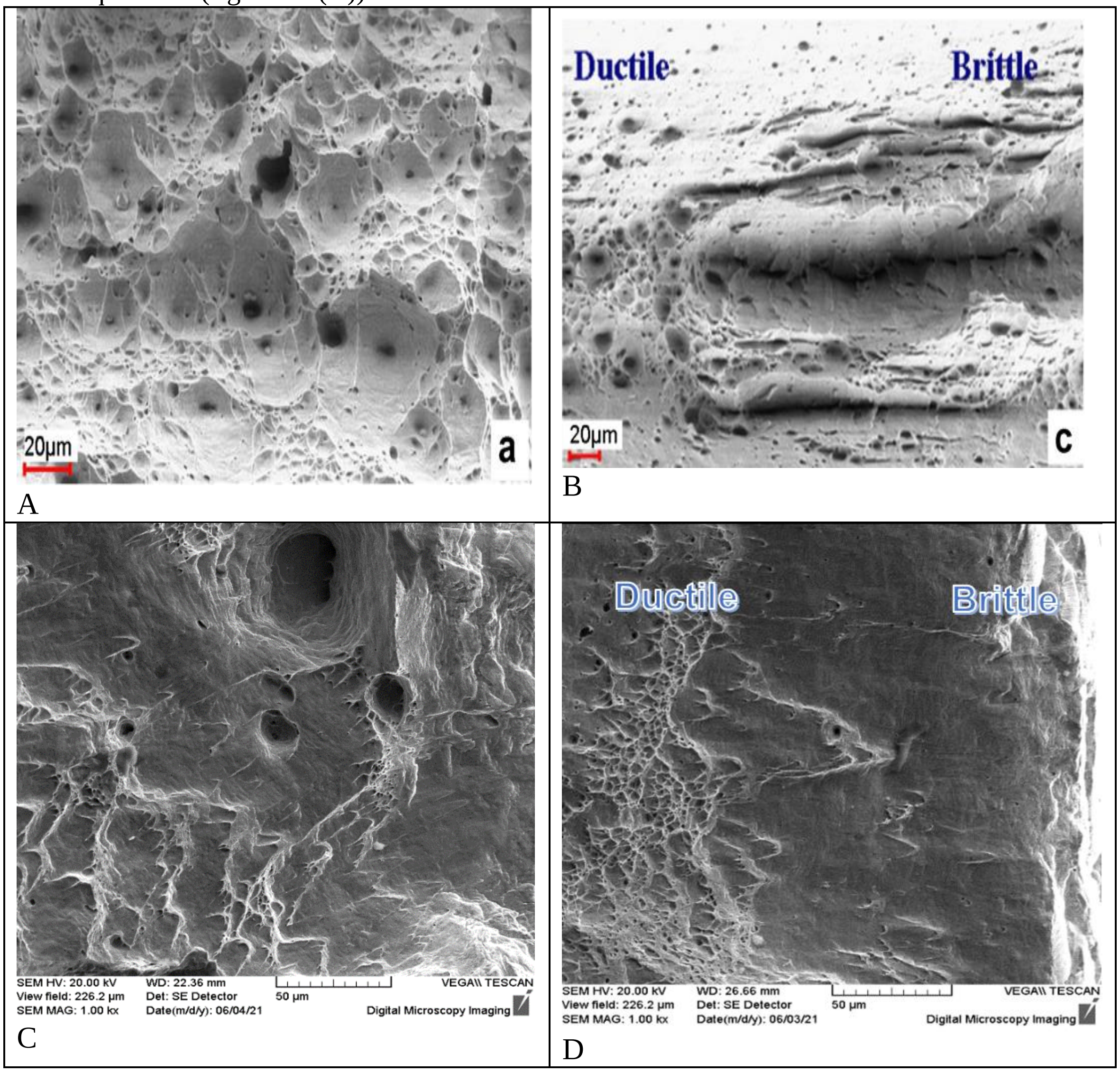

Figure 24. *SEM analyzes of breaking surfaces: (A) air, 160 ℃, [12]; (B) LBE 160 ℃ [12]; (C) air, 375 ℃ - this paper; (D) liquid lead, 375 ℃ - present work*

Given the above analysis, it is clear that the weakening effect of LME-type on the mechanical behaviour of 316L liquid lead steel for the temperature range 350°C – 400°C cannot be neglected, especially at low deformation rates. All the more so, it is necessary to model this phenomenon within the constitutive equations of the mechanical stress-strain type, which would render as true as possible the behaviour of a structural component of 316L austenitic steel in the liquid lead. These types of equations are useful in finite element analyzes of the state of stresses and strains, as well as in fracture mechanics.

6. PARAMETRIC EVALUATION OF THE EMBRITTLEMENT PHENOMENON IN LIQUID LEAD ENVIRONMENT BY VALORIZATION OF EXPERIMENTAL RESULTS

Description of the method proposed in the doctoral study for obtaining the Ramberg – Osgood constitutive equation that models the elastic-plastic mechanical behaviour

An engineering stress-strain curve does not provide a true indication of the deformation characteristics of a metal. The curve known as the *true stress curve versus the true strain curve* is often also known as the flow curve because it is the basic characteristic of the plastic flow of the material [14].

True stress (σ) and true strain (ε) are defined as:

$$\sigma = \frac{P}{A_0}(1 + e) \tag{2}$$

$$\varepsilon = ln(1 + e) \tag{3}$$

$$e = \frac{\Delta L}{L_0} \tag{4}$$

where: P - instantaneous load (*N*); A_0 - the area of the original cross-section of the sample (*mm^2*); e - engineering strain; ΔL - total elongation of the sample (*mm*); L_0 - initial sample length (*mm*).

The mathematical relation that expresses the real mechanical stress-strain curve is a power-type curve [14], [15]. The Ramberg - Osgood plastic flow rule states that for quasi-static loading at a certain temperature and deformation rate, the true mechanical stress is given according to the coefficient of resistance K, the strain hardening exponent *n* and the true plastic deformation:

$$\sigma = K\varepsilon_p^n \tag{5}$$

where n - the hardening coefficient and K - the resistance coefficient.

Load instability in a sample is known as "necking deformation". Localized deformation generally begins at maximum load during tensile deformation of a ductile metal [14]. We can consider that mechanical stress is defined as:

$$P = \sigma \cdot A \tag{6}$$

Where *P*- is the mechanical load; σ - is the mechanical stress; *A* - cross-sectional area of the sample.

The state of instability that results in localized deformation is defined by the condition:

$$dP = \sigma \cdot dA + A \cdot d\sigma = 0 \tag{7}$$

From the constant volume condition for the sample:

$$\frac{dL}{L} = -\frac{dA}{A} \tag{8}$$

is obtained

$$-\frac{dA}{A} = \frac{dL}{L} = d\varepsilon_p \tag{9}$$

where ε it represents the mechanical deformation.

It follows from equation (7) with equation (9):

$$\frac{d\sigma}{\sigma} = d\varepsilon_p \text{ or } \frac{d\sigma}{d\varepsilon_p} = \sigma \tag{10}$$

From equation (5) we obtain:

$$\frac{d\sigma}{d\varepsilon_p} = nK\varepsilon_p^{n-1} \tag{11}$$

By combining equation (10) with equation (11) we have:

$$\sigma = nK\varepsilon^{n-1} \tag{12}$$

Mechanical deformation may be determined when localized deformation occurs:

$$\sigma = K\varepsilon_p^n = nK\varepsilon_p^{n-1} \tag{13}$$

This shows that the deformation at which the localized deformation occurs is numerically equal to the hardening coefficient of the deformation [14]:

$$\varepsilon_r = n \tag{14}$$

Based on this statement, this paper proposes a new method of obtaining the coefficient of hardening of the deformation, from the mechanical stress-strain curve.

Taking into account the relationship (14), in the doctoral study **a new method** for the hardening coefficient was **proposed** by solving the transcendental equation:

$$ln\left(\frac{\sigma_r}{\sigma_y}\right) = n\left[ln(n) - ln(\varepsilon_y)\right] \tag{15}$$

Equation (15) is solved numerically in the MATLAB programming environment [16]. Finally, the last format of the Ramberg - Osgood equation becomes:

$$\frac{\varepsilon}{\frac{\sigma_0}{E}} = \frac{\sigma}{\sigma_0} + \alpha \cdot \left(\frac{\sigma}{\sigma_0}\right)^{\frac{1}{n}} \text{ or } \frac{\varepsilon}{\varepsilon_0} = \frac{\sigma}{\sigma_0} + \alpha \cdot \left(\frac{\sigma}{\sigma_0}\right)^{\frac{1}{n}} \tag{16}$$

Equation Ramberg - Osgood (16) is completely determined if α and n are known. Solving equation (15), to obtain the strain hardening coefficient, n. In order to obtain α, in the doctoral study the equation is proposed:

$$\alpha = \frac{0.002 \cdot E}{\sigma_y} \tag{17}$$

For practical reasons, the parameters for mechanical stress-strain have been determined α, respectively $m = 1/n$, and the Ramberg - Osgood equation, from the format given by equation (16), which will be used in the finite element analysis software, has form:

$$\frac{\varepsilon}{\varepsilon_0} = \frac{\sigma}{\sigma_0} + \alpha \cdot \left(\frac{\sigma}{\sigma_0}\right)^m \tag{18}$$

Fracture mechanics software called FEACrack [17] in this paper uses the Ramberg-Osgood equation in the format given by relation 18.

Preliminary analysis of the experimental results obtained in the test matrix

Following the analysis and processing of the data from the traction curves, the results were obtained from the test matrix in air and liquid lead, respectively, presented in the doctoral thesis.

As noted, the two result matrices contain the following quantities:

- Yield stress $\sigma_{0.2}$;
- Ultimate tensile strength σ_r;
- The parameter α of the Ramberg - Osgood relationship;
- Parameter m, which is the reverse hardening coefficient, n.

Next, it is interesting to analyze the variation of the parameters presented in the two matrices of the results depending on the test temperature and the deformation rate used in the tensile tests. For this, a two-dimensional linear analysis using the MATLAB programming environment was preferred. Thus, in the following figures, the 3D surface of the dependence of the analyzed quantities will be exposed depending on the temperature and the deformation rate, as well as the bilinear interpolation equation.

For air, the graphical results are shown in Figures 25-28.

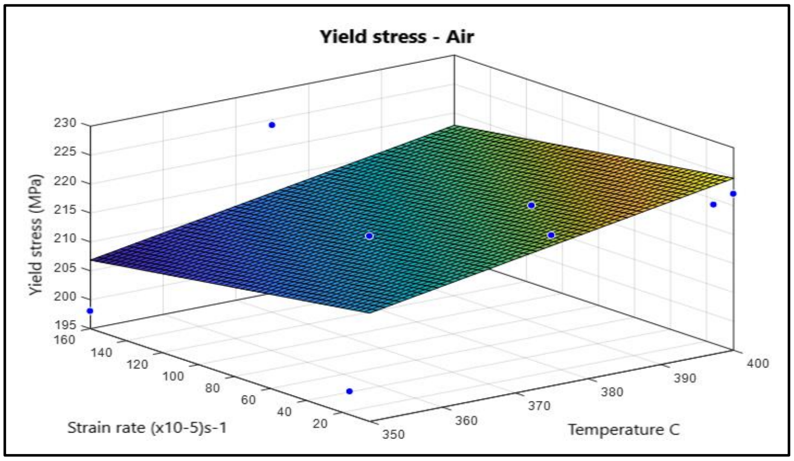

Model "Linear Poly11" (MATLAB): sf (x, y) = p00 + p10 * x + p01 * y; Coefficients (with 95% confidence interval): p00 = 137; p10 = 0.22; p01 = -0.04439

***Figure 25.** 316L austenitic steel yield stress variation with strain rate and air test temperature*

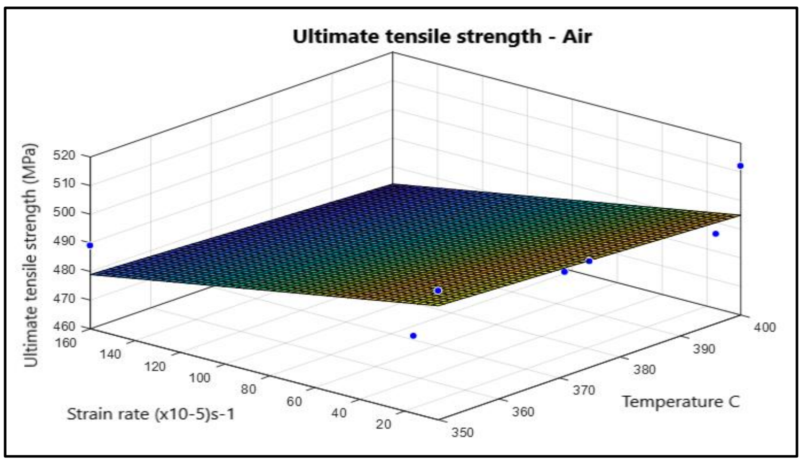

Poly11 Linear Model (MATLAB): sf (x, y) = p00 + p10 * x + p01 * y; Coefficients (with 95% confidence interval): p00 = 535.5; p10 = -0.1; p01 = -0.1349

***Figure 26.** 316L austenitic steel ultimate tensile strength variation with strain rate and air test temperature*

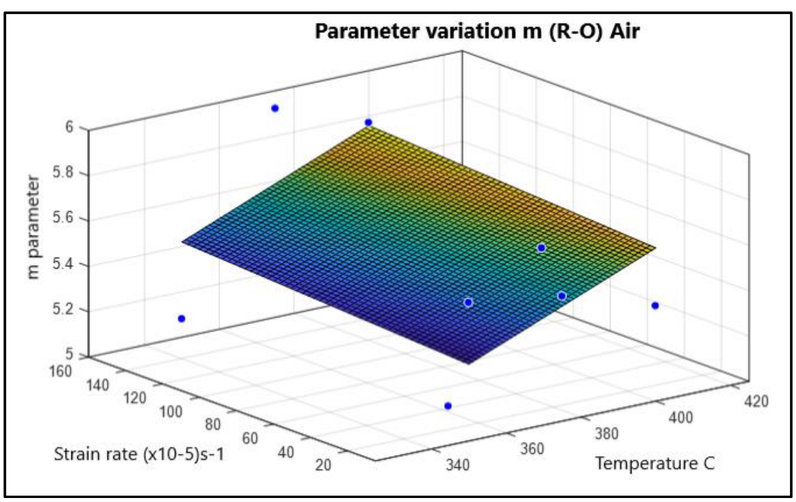

Poly11 Linear Model (MATLAB): sf (x, y) = p00 + p10 * x + p01 * y; Coefficients (with 95% confidence interval): p00 = 2.98; p10 = 0.006733; p01 = 0.0005207

***Figure 27.** 316L austenitic steel parameter variation m with deformation rate and air test temperature*

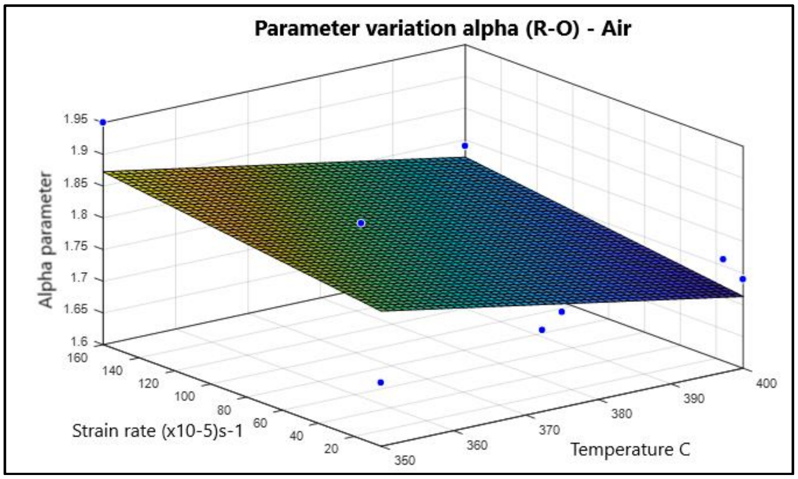

Poly11 Linear Model (MATLAB): sf (x, y) = p00 + p10 * x + p01 * y; Coefficients (with 95% confidence interval): p00 = 2,511; p10 = -0.002; p01 = 0.0003823

***Figure 28.** 316L austenitic steel parameter variation α with deformation rate and air test temperature*

For the yield stress (figure 25), the following tests are performed in the air:

- As the deformation rate increases, the flow limit values have a slight tendency to increase;
- As the test temperature increases, it is more obvious to increase the yield stress limit values.

For ultimate tensile strength (Figure 26), the following air tests are found:

- At a temperature of 350ºC the ultimate tensile strength remains almost constant with the increase of the deformation rate; at a temperature of 400ºC the values of the ultimate tensile strength have an obvious increase when the deformation rate increases;
- At low deformation rates the ultimate tensile strength decreases with increasing temperature, and at high deformation rates, the process is reversed.

For the Ramberg - Osgood equation parameter m (Figure 27), the following air tests are observed:

- For the whole temperature range (350ºC – 400ºC), the value of the parameter m decreases slightly with the increasing rate of deformation;
- As the temperature increases, regardless of the deformation rate, the value of the parameter increases.

For the Ramberg - Osgood equation parameter α (Figure 28), the following air tests are found:

- For the whole temperature range (350ºC – 400ºC), the value of the parameter α decreases slightly with increasing deformation speed;
- As the temperature increases, regardless of the deformation rate, the value of the parameter decreases.

For the tests performed in a liquid lead, the graphical results are shown in Figures 29 - 32.

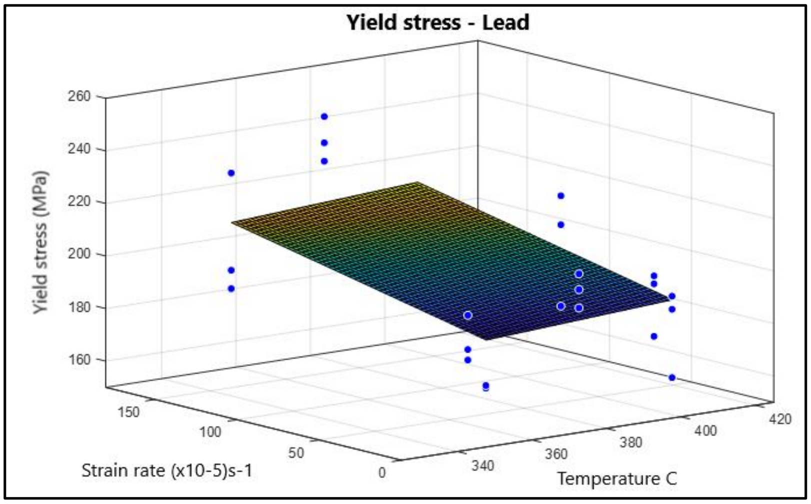

Poly11 Linear Model (MATLAB): sf (x, y) = p00 + p10 * x + p01 * y; Coefficients (with 95% confidence interval): p00 = 158.5; p10 = 0.08667; p01 = 0.1343

Figure 29. *316L austenitic steel yield stress variation with deformation rate and test temperature in liquid lead*

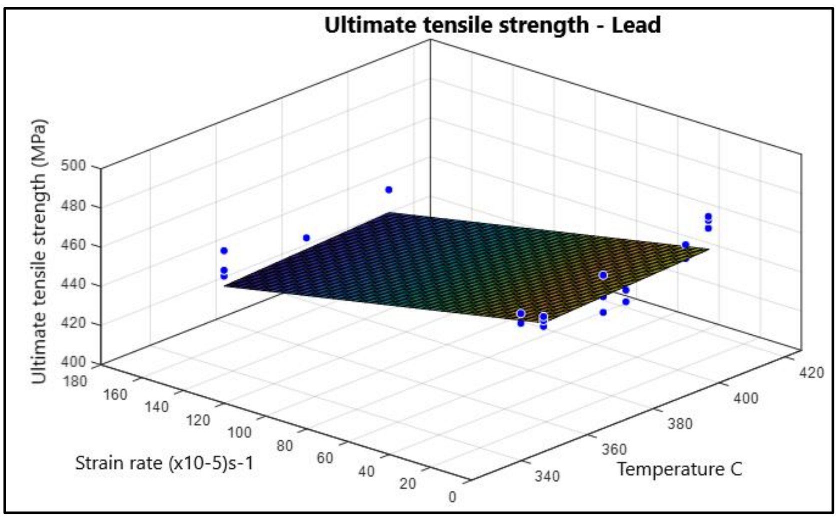

Poly11 Linear Model (MATLAB): sf (x, y) = p00 + p10 * x + p01 * y; Coefficients (with 95% confidence interval): p00 = 432.8; p10 = 0.08667; p01 = -0.2061

Figure 30. *Variation of ultimate tensile strength of 316L austenitic steel with deformation rate and test temperature in liquid lead*

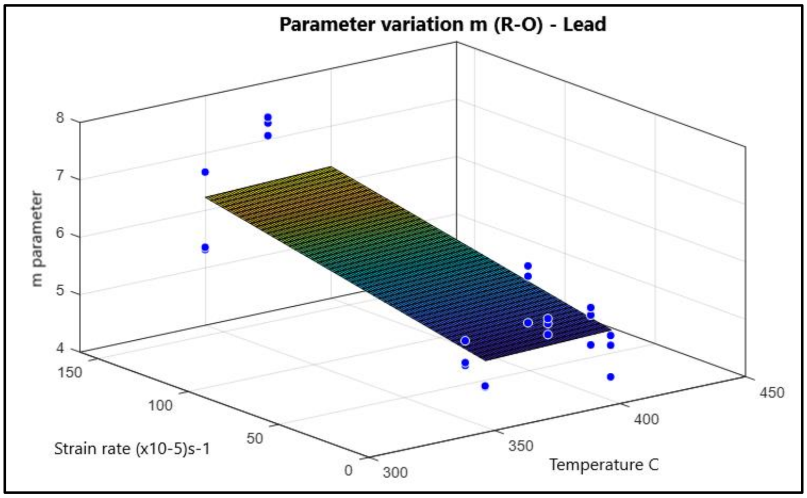

Poly11 Linear Model (MATLAB): sf (x, y) = p00 + p10 * x + p01 * y; Coefficients (with 95% confidence interval): p00 = 4,665; p10 = 0.001311; p01 = 0.006887

Figure 31. *Parameter variation m of austenitic 316L steel with strain rate and test temperature in liquid lead*

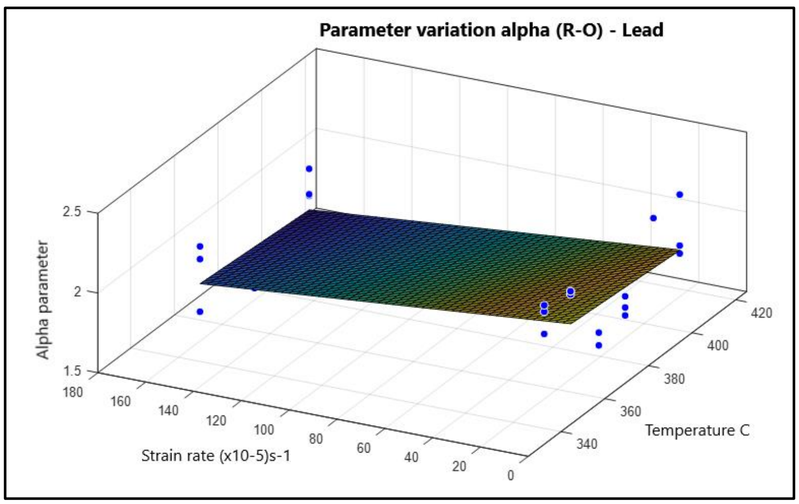

Poly11 Linear Model (MATLAB): sf (x, y) = p00 + p10 * x + p01 * y; Coefficients (with 95% confidence interval): p00 = 2,446; p10 = -0.001089; p01 = -0.001288

Figure 32. *Parameter variation α of 316L austenitic steel with strain rate and test temperature in liquid lead*

From the examination of the graphs in figures 29 - 32, it can be seen a consistent spread of the values of the analyzed parameters, this being a normal thing because the aspects of the influence of the liquid lead on the thermomechanical characteristics of traction are quite complex. At the same time, the performance of liquid lead tensile tests, monitoring and data acquisition are difficult, so this scattering of experimental data can be seen as an intrinsic feature of this type of test. With the help of the two-dimensional linear representation, however, certain conclusions can be drawn for the analyzed parameters.

For the yield stress (figure 29), the tests performed in liquid lead show the following:

- For the whole temperature range (350 ºC – 400 ºC), the value of the flow limit decreases with increasing deformation rate;
- On the other hand, regardless of the value of the deformation rate, with the increase of the test temperature, the value of the yield stress slightly increases.

For ultimate tensile strength (Figure 30), the following tests are performed on liquid lead:

- For the whole temperature range (350 ºC - 400 ºC), the value of the ultimate tensile strength increases with the increase of the deformation rate;
- Conversely, regardless of the value of the deformation rate, the ultimate tensile strength increases slightly with increasing test temperature.

For the Ramberg - Osgood equation parameter m (Figure 31), the liquid lead tests show:

- For the whole temperature range (350 ◦ C - 400 ◦ C), the value of the parameter m decreases significantly with the increase of the deformation rate;
- As the temperature increases, the value of the parameter m remains almost constant for a given value of the strain rate.

For the Ramberg - Osgood equation parameter α (Figure 32), the following tests are performed on liquid lead:

- For the whole temperature range (350 ºC – 400 ºC), the value of the parameter α remains almost constant at each value of the deformation rate;
- The same can be said for the dependence on the rate of deformation at a certain temperature value.

Proposed parametric equations for modelling Ramberg-Osgood constitutive behaviour using the artificial neural network method

In the doctoral study, the Ramberg - Osgood constitutive equation was modelled using the parameters α and $m = 1/n$, so that this model contains the dependence of these parameters on the following four variables:

- Yield stress $\sigma_{0.2}$;
- Ultimate tensile strength σ_r;
- The parameter α of the Ramberg - Osgood relationship;
- Parameter m, which is the reverse hardening coefficient, *n*.

This will allow the use of the Ramberg - Osgood equation in finite element method analyzes, especially where nonlinear (elastic-plastic) relationships between mechanical stresses and strains occur. Thus, in the structural integrity analysis, where the state of stresses and deformations in the area of defects (cracks) is followed, the relations of mechanical stress - deformation are in the field that exceeds the yield stress. At the same time, the model developed in the doctoral study will allow the practical use of the Ramberg - Osgood relationship without the user having to solve the transcendental equation separately to obtain the hardening coefficient of deformation.

The general stages of the construction, training and validation of the MFNN neural network model were analyzed and characterized in the chapters of the doctoral thesis.

Artificial neural network modelling is radically different from mathematical modelling. The behavioural information contained in the experimental databases is used directly by the constitutive neural models. For these constitutive models in the methodology of artificial neural networks no need for idealizations, as is normally done in mathematical modelling. Therefore, the methodology of artificial neural networks allows the description of quite complex relationships, for example, between mechanical stresses and deformations.

The neural network methodology can be applied in any situation where a relationship between *input* variables and predicted *output* variables is required. This can be done even if the relationship is very complex. In the approximation of functions, two neural networks are the most used, namely: Multilayer Feedforward Neural Network (MFNN) and Radial Basis Function (RBF). The MFNN network is probably the most popular network architecture used today in nonlinear neural modelling. In this type of network, each unit performs a weighted amount of *input* data and passes this activation level through a transfer function.

The "Multilayer Feedforward Neural Network" (abbreviated MFNN), with the following approximate translation "Unidirectional Multilayer Neuronal Network", is an important class of artificial neural networks. This type of network consists of a set of source nodes, which constitute the input, one or more hidden layers with the computing nodes, and an output layer, which constitutes the output layer with computing nodes [18]. Input data is processed through a one-way network, "forward", passing through successive layers. The MFNN abbreviation will continue to be used for this type of network.

The general stages of the construction, training and validation of the MFNN neural network model were analyzed in the thesis. Such a model will be used in the paper to evaluate the parameters α and $m = 1/n$ what characterizes the constitutive equation Ramberg - Osgood. The model is based on the two matrices of the results obtained from the tensile tests performed in the air environment, respectively the liquid lead environment.

The MFNN neural network model will contain two layers of neurons. We will work with 5 neurons for the hidden layer, and for the output layer, we will use only one neuron. This model can accept several variables as input and the sketch of the MFNN model was shown in Figure 33.

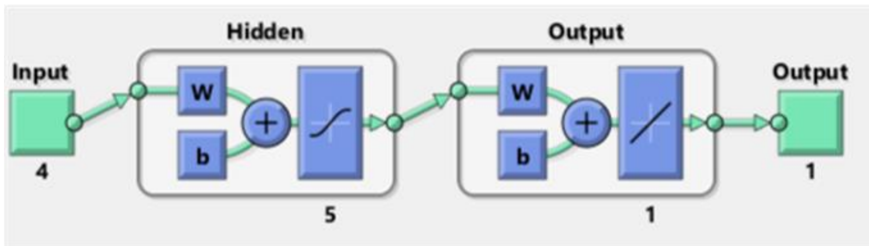

Figure 33. *Matlab icon of the MFNN network built in the doctoral study*

The MFNN model built in the work for the parameters α and $m = 1/n$, which characterizes the constitutive equation Ramberg - Osgood, accepts as input the following variables: ***temperature, deformation rate in traction, yield stress, ultimate tensile strength***. Also, when other test characterization parameters (oxygen concentration, etc.) are available, they can be used as components of the input vector. For this model, the output values are the estimated values of the parameters α and $m = 1/n$ what characterizes the Ramberg - Osgood constitutive equation. For the hidden layer we used the *tansig* transfer function, and for the output layer the *purelin* transfer *function.*

Obtaining explicit functions for parameters α and m through the MFNN network model

Using the methodology of the artificial neural method mentioned above, will be obtained explicit functions of the parameters α and m on the basis of test data contained in the matrix in the liquid lead and air environments.

For air

The input data in the test matrix are: ***temperature, strain rate, yield stress, ultimate tensile strength.*** Output values are parameter values α.

Following data processing, the function has the following form:

$$\begin{aligned}\alpha_{air}(T,\dot{\varepsilon},\sigma_{0.2},\sigma_r) == {} & \frac{0.1535199832}{\exp(0.0157169072\cdot\sigma_{0.2} - 0.06676656384\cdot\sigma_r - 0.07362022963\cdot T - 0.1083065326\cdot\dot{\varepsilon} + 75.29003156) + 1.0} \\ & - \frac{0.2365077134}{\exp(0.04264235719\cdot\sigma_r - 0.4544772243\cdot\sigma_{0.2} - 0.00392211372\cdot T - 0.008434048107\cdot\dot{\varepsilon} + 79.34997665) + 1.0} \\ & + \frac{0.6325132439}{\exp(50.14925053 - 0.07986180668\cdot\sigma_r - 0.234652205\cdot T - 0.05375160671\cdot\dot{\varepsilon} - 0.03426597872\cdot\sigma_{0.2}) + 1.0} \\ & - \frac{2.076965747}{\exp(0.5050429755\cdot\sigma_{0.2} + 0.2481844408\cdot\sigma_r - 0.3889452763\cdot T + 0.2070418955\cdot\dot{\varepsilon} - 49.10719742) + 1.0} \\ & - \frac{2.153155082}{\exp(0.2180445427\cdot\sigma_{0.2} + 0.1479708912\cdot\sigma_r + 0.1207130135\cdot T + 0.07089952978\cdot\dot{\varepsilon} - 123.4715136) + 1.0} \\ & + 1.307553795\end{aligned} \tag{19}$$

The prediction of the function $\alpha_{air}(T,\dot{\varepsilon},\sigma_{0.2},\sigma_r)$ is represented in figure 34, where a good concordance with the corresponding values from the test matrix can be found.

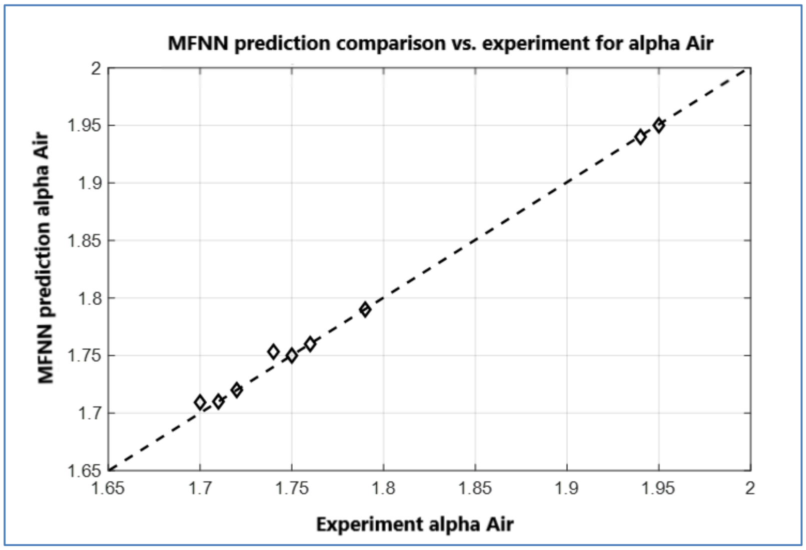

Figure 34. *Prediction of function* $\alpha_{air}\ (T, \dot{\varepsilon}, \sigma_{0.2}, \sigma_r)$ *vs. experimental values*

The programs were implemented in MATLAB to obtain the other functions specific to the Ramberg - Osgood parameters.

For the parameter $m_{air}(T, \dot{\varepsilon}, \sigma_{0.2}, \sigma_r)$ the MFNN function is:

$$
\begin{aligned}
m_{air}(T, \dot{\varepsilon}, \sigma_{0.2}, \sigma_r) &= \\
&= \frac{1.376823648}{\exp(0.1010589155 \cdot \sigma_r - 0.00903922038 \cdot \sigma_{0.2} - 0.1437156176 \cdot T + 0.01072826591 \cdot \dot{\varepsilon} - 23.45732203) + 1.0} \\
&- \frac{2.290502637}{\exp(0.1350483712 \cdot T - 0.03574108429 \cdot \sigma_r - 0.1594679465 \cdot \sigma_{0.2} - 0.02427346108 \cdot \dot{\varepsilon} + 32.53306723) + 1.0} \\
&- \frac{3.027996311}{\exp(0.09500214958 \cdot T - 0.05144939472 \cdot \sigma_r - 0.265195393 \cdot \sigma_{0.2} + 0.05112680995 \cdot \dot{\varepsilon} + 78.1810692) + 1.0} \\
&- \frac{2.71534429}{\exp(0.1816733758 \cdot T - 0.1041205667 \cdot \sigma_r - 0.09708069808 \cdot \sigma_{0.2} - 0.1315849855 \cdot \dot{\varepsilon} + 48.45071035) + 1.0} \\
&+ \frac{2.041644833}{\exp(0.02508797134 \cdot \sigma_r - 0.05717042737 \cdot \sigma_{0.2} - 0.0004544975416 \cdot T - 0.00004444304224 \cdot \dot{\varepsilon} + 1.064443306) + 1.0} \\
&+ 3.508276934
\end{aligned} \tag{20}
$$

The prediction of the function $m_{air}\ (T, \dot{\varepsilon}, \sigma_{0.2}, \sigma_r)$ is represented in figure 35, where a good agreement with the corresponding values in the test matrix can also be found.

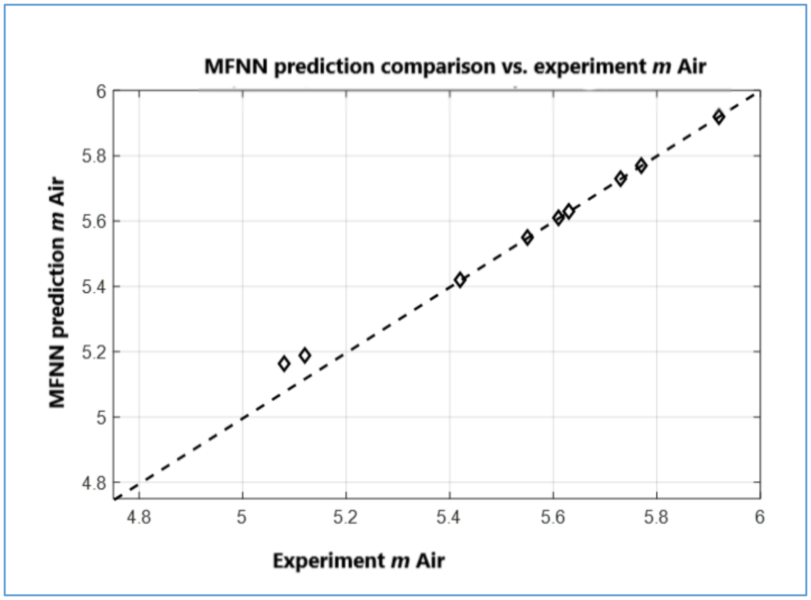

Figure 35. *Prediction of function* $m_{air}\ (T, \dot{\varepsilon}, \sigma_{0.2}, \sigma_r)$*vs. experimental values*

For lead:

For the analysis of the test results performed in the liquid lead environment, programs implemented in MATLAB were made with the input parameters from the test matrix.

Thus, for the parameter $\alpha_{lead}(T, \dot{\varepsilon}, \sigma_{0.2}, \sigma_r)$ the corresponding MFNN function is:

$$\begin{aligned}
&\alpha_{lead}(T, \dot{\varepsilon}, \sigma_{0.2}, \sigma_r) = \\
&= \frac{0.01111703549}{\exp(0.1758779686 \cdot \sigma_{0.2} - 0.6841160186 \cdot \sigma_r + 0.4240382537 \cdot T + 0.4211538564 \cdot \dot{\varepsilon} + 73.75522087) + 1.0} \\
&- \frac{0.4168912674}{\exp(0.4670985643 \cdot \sigma_{0.2} - 0.0421241148 \cdot \sigma_r + 0.3415910184 \cdot T - 0.3131816471 \cdot \dot{\varepsilon} + 19.93870722) + 1.0} \\
&+ \frac{0.9591262485}{\exp(0.04809159409 \cdot \sigma_{0.2} + 0.003358524713 \cdot \sigma_r - 0.0005350602848 \cdot T + 0.0004271396583 \cdot \dot{\varepsilon} - 10.41126806) + 1.0} \\
&+ \frac{0.04771190512}{\exp(1.005654552 \cdot \sigma_{0.2} - 0.4563315874 \cdot \sigma_r - 0.1039207902 \cdot T - 0.0006274577723 \cdot \dot{\varepsilon} - 59.20988646) + 1.0} \\
&+ \frac{1.71252668}{\exp(0.4536180027 \cdot \sigma_r - 0.1283652688 \cdot \sigma_{0.2} - 0.4198358056 \cdot T - 0.01257380184 \cdot \dot{\varepsilon} - 56.939743) + 1.0} - 0.195416497
\end{aligned} \tag{21}$$

The intercomparison of prediction $\alpha_{lead}(T, \dot{\varepsilon}, \sigma_{0.2}, \sigma_r)$ versus experiment is shown in Figure 36.

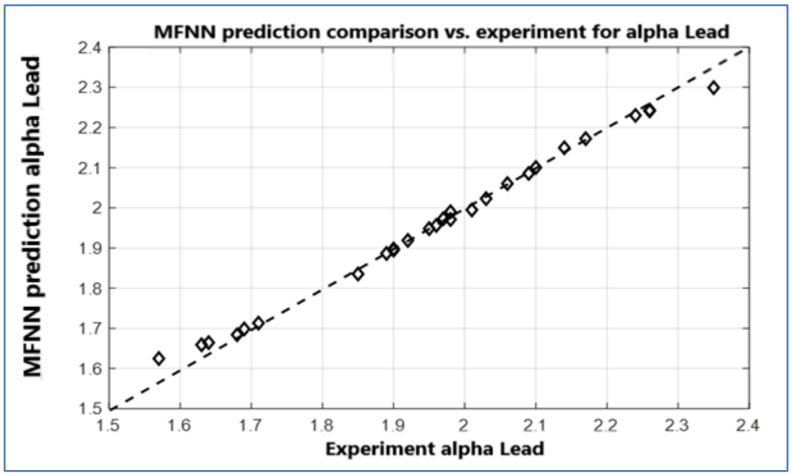

Figure 36. *Prediction of function* $\alpha_{plumb}(T, \dot{\varepsilon}, \sigma_{0.2}, \sigma_r)$*vs. experiment values*

For the parameter $m_{lead}\,(T, \dot{\varepsilon}, \sigma_{0.2}, \sigma_r)$ the MFNN function is:

$$
\begin{aligned}
& m_{lead}\,(T, \dot{\varepsilon}, \sigma_{0.2}, \sigma_r) = \\
&= \frac{3.643881706}{\exp(0.6385643297 \cdot T \,-\, 0.2022424958 \cdot \sigma_r \,-\, 0.6227643831 \cdot \sigma_{0.2} \,-\, 0.1053848883 \cdot \dot{\varepsilon} \,-\, 77.21535061) + 1.0} \\
&- \frac{9.884337419}{\exp(0.01629318253 \cdot \sigma_{0.2} \,-\, 0.007234343592 \cdot \sigma_r + 0.0007329634094 \cdot T \,+\, 0.0001456651298 \cdot \dot{\varepsilon} \,-\, 1.455770771) + 1.0} \\
&+ \frac{0.08146039906}{\exp(0.4112705698 \cdot \sigma_{0.2} \,-\, 0.3970669265 \cdot \sigma_r \,-\, 0.3081988387 \cdot T \,+\, 0.3491973275 \cdot \dot{\varepsilon} \,+\, 38.95247934) + 1.0} \\
&+ \frac{7.106945027}{\exp(0.4026283571 \cdot \sigma_{0.2} \,+\, 0.4217960215 \cdot \sigma_r \,-\, 0.8012441872 \cdot T \,+\, 0.07559427212 \cdot \dot{\varepsilon} \,-\, 37.3985282) + 1.0} \\
&+ \frac{1.621509654}{\exp(0.3513192334 \cdot \sigma_{0.2} \,+\, 0.09960028714 \cdot \sigma_r \,-\, 0.7307116249 \cdot T \,+\, 0.2176743567 \cdot \dot{\varepsilon} \,+\, 69.50970479) + 1.0} + 0.6084863663
\end{aligned}
\tag{22}
$$

Figure 37 shows the intercomparison of the values predicted by the function $m_{lead}\,(T, \dot{\varepsilon}, \sigma_{0.2}, \sigma_r)$ with those resulting from the experiment.

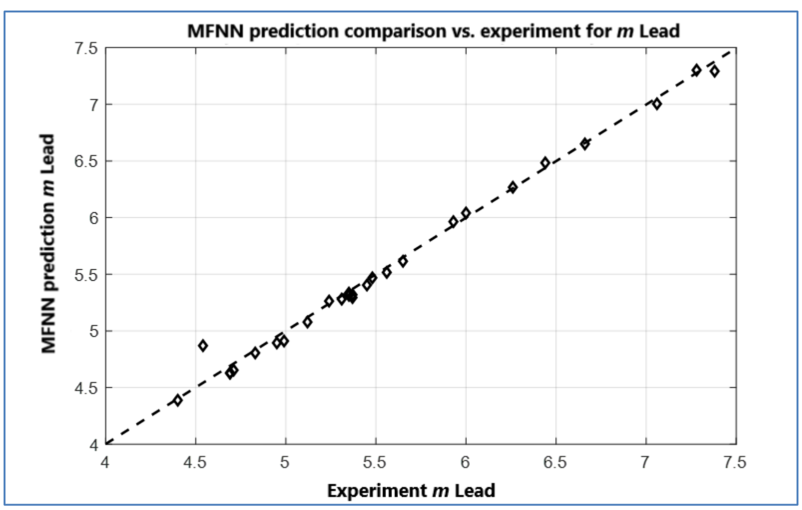

Figure 37. *Prediction of function* $m_{lead}\,(T, \dot{\varepsilon}, \sigma_{0.2}, \sigma_r)$ *vs. experiment values*

Some comments are needed on the predictive accuracy of the MFNN model for the values α and m compared to the experiments performed in the liquid lead environment. The preliminary analysis found a considerable spread for the parameter values: flow limit, breaking strength, calculated parameter values α and m. This fact was further highlighted in the two-dimensional linear representation, Figures 29-32. However, the modelling by the method of artificial neural networks of MFNN type leads to obtaining quite accurate prediction functions for α and m, a remarkable fact especially since they are based on four modeling parameters: ***temperature, deformation rate, yield stress, ultimate tensile strength.*** Such modelling, in which to enter several input parameters is very difficult to achieve by the usual fitting methods with which the statistical packages from various programs are provided.

Valorization of the results of own research from the doctoral study within an application of rupture mechanics

In structural integrity analyzes performed using finite element method programs (eg ANSYS, ABAQUS) it is necessary to specify the constituent equations of material as a mandatory input requirement.

In the doctoral thesis, an application of the research is presented by using the Ramberg - Osgood equation with parameters obtained in the paper for an analysis of the mechanics of rupture. This analysis envisages the initiation and propagation of a crack in 316L austenitic steel in the liquid lead environment. The analysis will be performed with the breaking mechanics software, FEACrack [17], which uses the finite element method to analyze the mechanical stress field in the material, and the crack initiation and propagation process is based on the Gurson-Tvergaard-Needleman (GTN) model [19],[20]. In the application of fracture mechanics in this study, the GTN model will be configured to describe the initiation and propagation of cracks on CT (Compact Tension) samples, having the specific characteristics of 316L steel obtained in the doctoral study by low deformation tensile tests (SSRT), in air and liquid lead media.

From the test matrix, we will use SSRT tests in air and liquid lead. From the equations obtained for the parameters of the Ramberg - Osgood relation, we will obtain the numerical values for the analyzed situation.

For tests performed in the air we apply the conditions:

- Temperature 400 (*units* ^oC);
- Strain rate $\dot{\varepsilon} = 5\ (units\ 10^{-5}\ s^{-1})$;
- Yield stress $\sigma_{0.2} = 222\ (units\ MPa)$;
- Ultimate tensile strength $\sigma_r = 512\ (units\ MPa)$

Using the equation for the α parameter obtained in the MFNN (equation 19) we obtain:

$$\alpha_{air}\ (T, \dot{\varepsilon}, \sigma_{0.2}, \sigma_r) = \alpha_{air}\ (400, 5, 222, 512) = 1.75 \qquad (23)$$

Analogous to the m coefficient (equation 20) we obtain:

$$m_{air}\ (T, \dot{\varepsilon}, \sigma_{0.2}, \sigma_r) = m_{air}\ (400, 5, 222, 512) = 5.42 \qquad (24)$$

Thus, in the air, the constitutive equation Ramberg - Osgood to 316 to 400ºC is:

$$\frac{\varepsilon}{\varepsilon_0} = \frac{\sigma}{\sigma_0} + 1.75 \cdot \left(\frac{\sigma}{\sigma_0}\right)^{5.42} \qquad (25)$$

With the ASTM E646-07 approach [21] for the coefficient of deformation hardening, for tests in the air environment, the value is $m = 4.1$ of the same order of magnitude as that obtained above. It should also be noted that the ASTM E646-07 mentions an error in the results between 5% and 15%.

To verify the accuracy of the prediction given by Equation 25, Figure 38 shows a comparison between the experimental mechanical stress-strain curve and Equation 25 for the air environment.

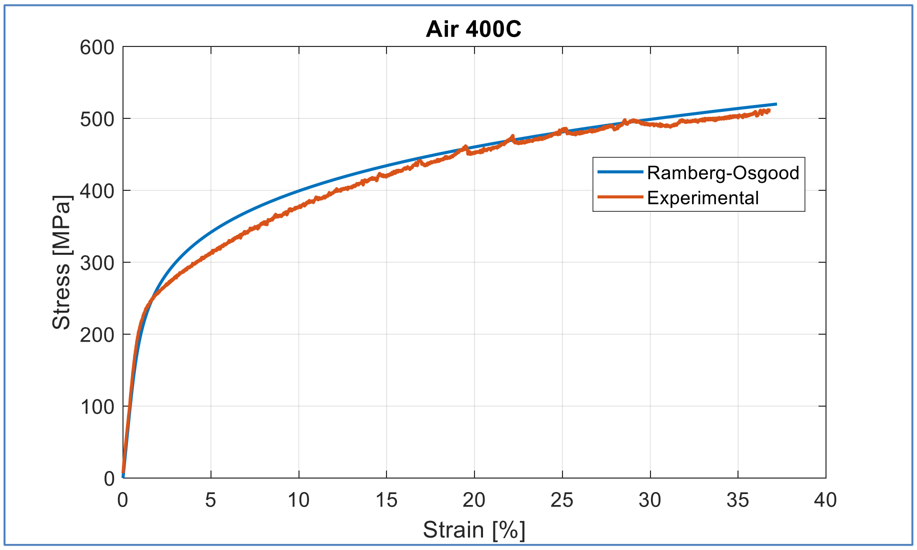

Figure 38. *Comparison between experimental and Ramberg - Osgood stress-strain relationships for SSRT in the air at 400 ℃*

For tests performed in the liquid lead environment we apply the conditions:

- Temperature 400 (*units ℃*);
- Strain rate $\dot{\varepsilon} = 5(units\ 10^{-5}\ s^{-1})$;
- Yield stress $\sigma_{0.2} = 208\ (units\ MPa)$;
- Ultimate tensile strength $\sigma_r = 483\ (units\ MPa)$.

Using the equation for the α parameter obtained in the MFNN (equation 21) we obtain:

$$\alpha_{lead}\ (T, \dot{\varepsilon}, \sigma_{0.2}, \sigma_r) = \alpha_{lead}\ (400, 5, 208, 483) = 1.83 \qquad (26)$$

Analogous to the m coefficient (equation 22) we obtain:

$$m_{lead}\ (T, \dot{\varepsilon}, \sigma_{0.2}, \sigma_r) = m_{lead}\ (400, 5, 208, 483) = 5.35 \qquad (27)$$

In the liquid lead, constitutive equation Ramberg - Osgood for 316L stainless steel, 400 °C becomes:

$$\frac{\varepsilon}{\varepsilon_0} = \frac{\sigma}{\sigma_0} + 1.83 \cdot \left(\frac{\sigma}{\sigma_0}\right)^{5.35} \qquad (28)$$

With the same approach as ASTM E646-07, for the hardening coefficient, for the tests in the liquid lead environment, the value is $m = 3.4$ of the same order of magnitude as that obtained above.

Figure 39 shows a comparison between the experimental mechanical stress-strain curve and equation 28 for the liquid lead environment.

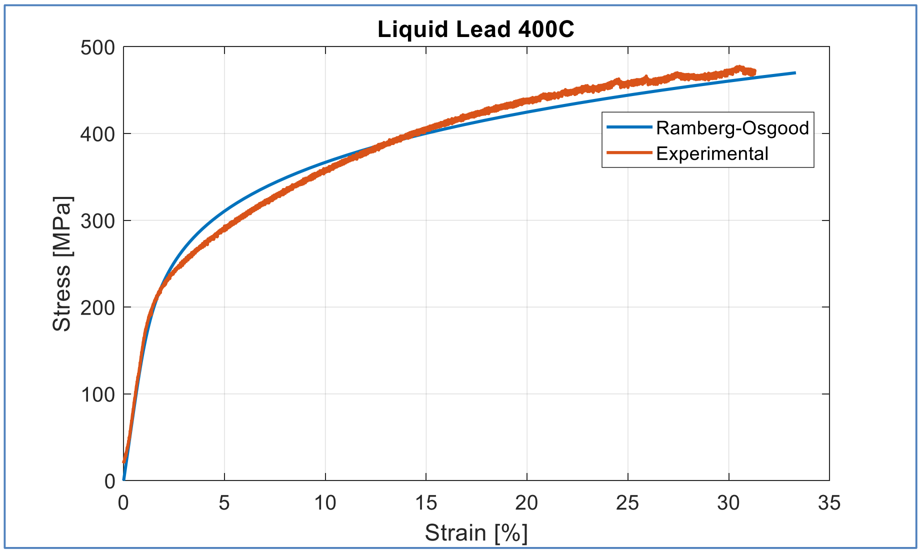

Figure 39. *Comparison between experimental and Ramberg Osgood stress-strain relationships for SSRT in the liquid lead at 400℃*

Analysis of the initiation and propagation of a crack by the finite element method uses a Compact-Tension (CT) test model, which is recommended by ASTM E1820 [22]. To determine the tensile strength properties of the material and *J*-integral. The CT model is implemented in the fracture mechanics software, called FEACrack [17], with the Ramberg-Osgood parameters mentioned above, and the model has the specific shape and dimensions as mentioned in ASTM E1820 (Figure 40).

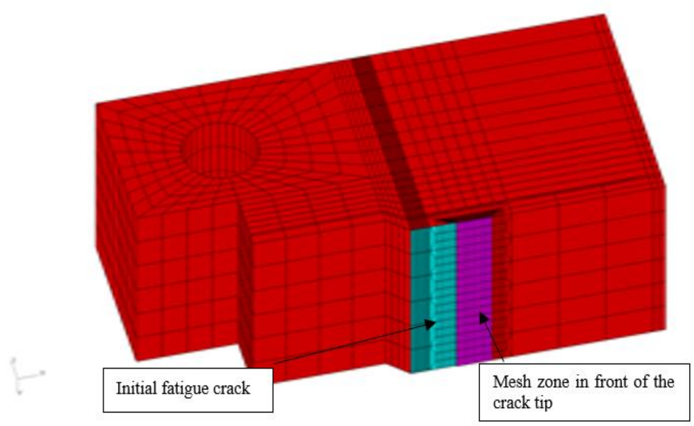

Figure 40. *CT sample model (half) and finite element mesh around the crack tip*

The analyzes are performed in the elastic-plastic field of mechanical stress. Therefore, to achieve the convergence of solutions for mechanical stress and strain, several application sequences of mechanical stress are required. Load control is preferred for load loading, as suggested by ASTM E1820.

To perform crack initiation and propagation, the model considers the extinction of finite elements in front of the crack front. This is achieved by de-cohesion when the critical porosity of the gaps in the finite elements of the region is reached. The extinction of the finite elements in front of the crack front leads to its advancement and this is repeated whenever the critical values of the fraction of gaps in the respective elements are realized.

The fracture mechanics analyzes performed with the FEACrack software, by the finite element method of the CT sample, using the modelling characteristics of the CT sample, will be interpreted further. Thus, for the analysis corresponding to the properties in the air test environment, figure 41 shows the state of the crack front after 60 loading steps. Its "tunnelling" shape is typical for cracking the CT sample under tensile load, which is always revealed in experimental tests of fracture mechanics.

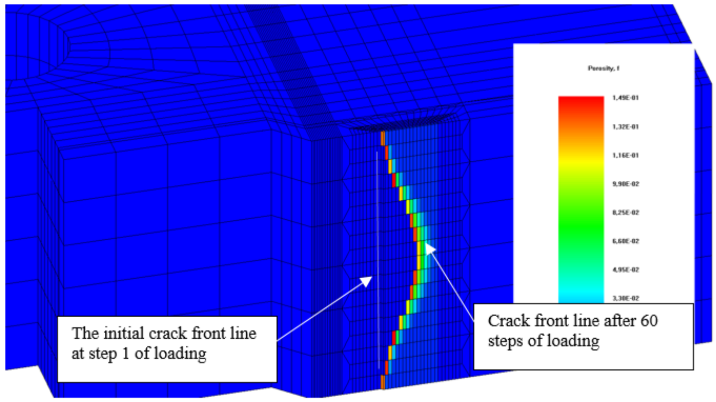

Figure 41. *The frontal shape of the crack after 60 loading steps (air)*

The same analyzes for the CT sample, using the test properties in the liquid lead environment, show the state of the crack front after 60 loading steps in Figure 42. In this case, too, the typical tunnelling pattern observed in the microscopy analyzes is found optics performed on experimentally tested CT samples.

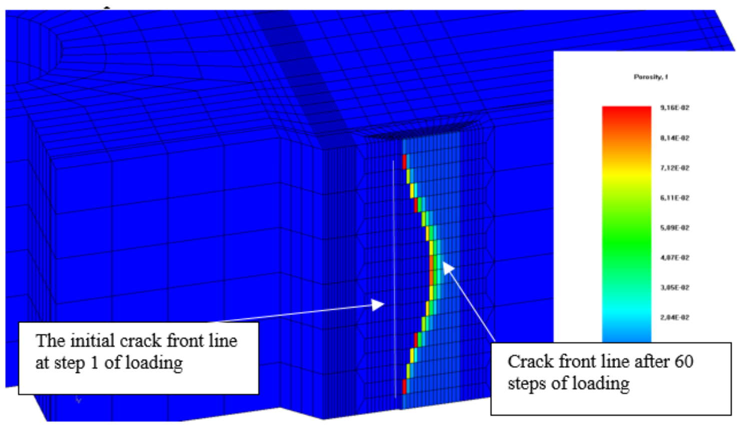

Figure 42. *The frontal shape of the crack after 60 loading steps (liquid lead)*

An image telling the LME-type response to the embrittlement of the liquid lead 400°C for crack growth simulation model 316 is shown in Figure 43.

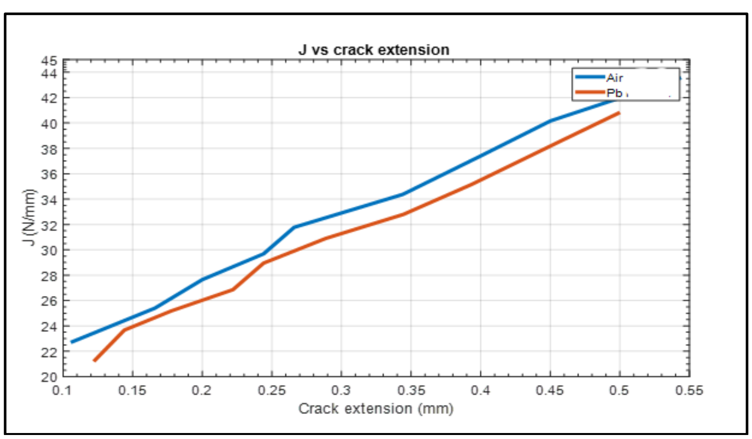

Figure 43.*Integral J versus crack extension in the liquid lead environment compared to the air environment*

The extension of the crack in the liquid lead is greater than the extension of the crack in the air at the same value of the *J*-integral. This is valid for the entire load range, which in this spectrum *J* integral values.

The following main observations can be made:

- at the same crack extensions, the corresponding values of the *J* integral are lower in liquid lead than in the air; this is in line with the fact that the Ultimate tensile strength (UTS) decreases by 7-8% in the liquid lead compared to the air tests; the same was mentioned in the reference [23] for the tensile strength for the steel LBE 316L (Bismuth Eutectic Liquid) at 200ºC and 300ºC;
- at the same values of the *J* integral, the extensions of the cracks in the liquid lead are higher by about 10-15%; this is consistent with the fact that the deformation at break decreases by 13-14% in the liquid lead compared to experimental SSRT tests performed in the air.

These observations demonstrate that ***the parametric model*** developed in the doctoral study has a great practical utility. It is developed for 316L steel, can simulate the mechanical behaviour of cracking in LME conditions in the liquid lead at 400ºC and the results are consistent with the results of experimental tests but also with similar ones mentioned in the literature [23, 24].

In this context, it should be noted that in reference [24] the different behaviour of the lead environment from the air environment is within the statistical field of experimental errors. However, the arguments of this doctoral study, presented above suggest that these differences exist and can be highlighted analytically, as was done in the doctoral approach.

The model is practical and will be used in the structural integrity activities of the innovative materials that will be used in the ALFRED demonstrator, which will be built at RATEN ICN Pitesti, Romania.

Characterization of the novelty and originality aspects of the parametric modelling performed in the doctoral study

I. The first aspect of **novelty** is the **performance of experimental tensile tests on samples of austenitic 316L stainless steel, in the liquid lead and the air**, to characterize the influence of liquid lead embrittlement on the thermomechanical behaviour in the temperature range 350ºC – 400ºC, the specific operating mode of the ALFRED demonstrator.
II. Another aspect of **novelty** is the **method of obtaining the coefficients α and m the constitutive equation defining the Ramberg - Osgood**, which characterizes the behaviour of the elastic-plastic ductile material under the application of uniaxial tension.
III. An **original feature** of the doctoral study is the **obtaining of an analytical model with practical utility, by processing the experimental results.** This is done by **using the method of the artificial neural network type** "**Multilayer Feedforward Neural Network**", (abbreviated **MFNN**) - in the MATLAB programming environment. This modern working method was proposed because the preliminary analysis of the experimental data showed a considerable spread for the parameter values: yield stress, ultimate tensile strength, calculated parameter values α and m. Thus, modelling by the method of artificial neural networks of MFNN type leads to obtaining quite accurate prediction functions for α and m. At the same time, it should be noted that the explicit MFNN type functions obtained have as input several important modelling parameters: temperature, strain rate, yield stress, ultimate tensile strength. This model also admits its further improvement with the accumulation of new experimental data as well as the knowledge of new parameters of influence (oxygen concentration in lead, etc.). Such modelling, in which to enter several input parameters is very difficult to achieve by the usual fitting methods with which the statistical packages from various programs are provided.
IV. Another **novelty** is the **application of fracture mechanics** described in the report, which uses the Ramberg - Osgood relationship with the coefficients rendered by explicit MFNN functions, to simulate the behaviour of cracking mechanics under LME conditions, in the liquid lead at 400ºC, as well as in the air, for 316L steel. For this, the micro-mechanical model of the Gurson-Tvergaard-Needleman ductile fracture was used. The model was implemented in the FEACrack fracture mechanics software, the stress

and strain analysis being performed by the finite element method. The obtained results are following the results of the experimental tests performed in the doctoral study but also with the similar ones mentioned in the literature.

V. The literature mentions the different mechanical behaviour in the liquid lead environment compared to the air environment of 316L steel, for the specified temperature range, being included in the statistical field of experimental errors. Instead, as a corollary of the novelty and originality aspects mentioned above, the arguments presented in the thesis suggest that these differences are real and can be highlighted analytically, as was done in the present doctoral study.

7. CONCLUSIONS OF THE DOCTORAL STUDY

Romania, through RATEN ICN, is involved in the construction of the ALFRED (Advanced Lead Fast Reactor European Demonstrator) demonstrator, which is based on cooling with liquid lead. This is one of the arguments for starting the studies within the doctoral thesis, with the stated objective on the issue of embrittlement of the structural materials specific to this type of reactor. Thus, the scientific approach of the doctoral thesis consists in highlighting the fragility induced by the contact of liquid lead - 316L steel, as well as its modelling by the equations constituting mechanical stress - deformation.

It should be noted that there are no systematic studies in the literature to assess the behaviour of mechanical tensile stress of 316L steel in the liquid lead environment, in the temperature range 350°C - 400°C. Therefore, the scientific approach of the doctoral study is all the more justified to elucidate the susceptibility of the LME phenomenon and to obtain the constitutive equations of material.

Below are the conclusions of the doctoral study, grouped into four topics: ***Motivation, Own Research, Analysis-Modelling, Application.***

MOTIVATION: Current status - Open issues

There are no systematic studies in the literature to evaluate the mechanical tensile stress of 316L steel in the liquid lead, in the temperature range 350°C - 400°C. Therefore, the scientific approach of the doctoral study focused on elucidating the susceptibility of the LME phenomenon and obtaining the constitutive equations of material.

In structural integrity analyzes performed using finite element method programs it is necessary to specify the constituent equations of material as a mandatory input requirement. When the analysis of the mechanical stress field is in the elastic-plastic field, the most used constitutive equation is Ramberg - Osgood. This becomes necessary when in the analyzed structural component there are discontinuities of material, initial defects or developed during operation, which constitute intensifiers of mechanical stress.

Within the analysis of the current scientific context, in the field in which the own researches of the doctoral study were carried out, the following were carried out:

- Analysis of the problem of using liquid lead used as a cooling agent in generation IV reactors;
- Critical analysis of the models elaborated in the speciality literature regarding the mechanisms of embrittlement with liquid metals.

Based on the mentioned analyzes, the objectives of the doctoral study were established, namely:

- Carrying out experimental comparative tensile tests in air and liquid lead media, on samples made of 316L steel, to highlight the LME mechanism determined by liquid lead;
- Carrying out an atlas of metallographic and SEM analyzes, on the samples resulting from the experimental tests, to highlight the cracking characteristics induced by the LME embrittlement of lead on 316L steel;
- Development of a new method for obtaining the parameters of the equation constituting mechanical stress - deformation, Ramberg - Osgood type, to use them in structural integrity analyzes;
- Development of a parametric model, based on artificial neural network, type "Unidirectional Multilayer Neuronal Network", to obtain analytical equations of the parameters of the Ramberg - Osgood equation, including the following parameters as input: temperature, strain rate, yield stress, ultimate tensile

strength. The model has practical utility in the analysis of the structural integrity of the various components of the ALFRED reactor;

- Development of an application of own research by using the Ramberg - Osgood equation with parameters obtained in the paper for an analysis of the fracture mechanics. This analysis envisages the initiation and propagation of a crack in 316L austenitic steel in the liquid lead environment. The analysis is performed with specialized fracture mechanics software, FEACrack, which uses the finite element method to analyze the mechanical stress field in the material, and the process of crack initiation and propagation is based on the Gurson-Tvergaard-Needleman (GTN) model.

OWN RESEARCH: Experiments - Results

Experimental tests were performed on samples of 316L stainless steel, used in Generation IV reactors as a structural material. These tensile tests were performed in both liquid lead and air. In this way, it was possible to better highlight the behaviour of the material under conditions of embrittlement due to the contact of steel-liquid lead. The experimental tensile tests were performed in air and liquid lead at three deformation rates and three temperatures of interest, according to ASTM E8/8M, respectively the SSRT type test according to ASTM - G129-00. The tensile curves mechanical stress-strain were processed according to the Ramberg - Osgood model.

As found, there is a significant influence of the LME effect on the traction of liquid lead in 316L austenitic steel samples, which is particularly noticeable at deformation rate $5 \times 10^{-5} s^{-1}$ (SSRT type), at all test temperatures (350°C, 375°C, 400°C).

Following the analysis and processing of the data from the traction curves, results were obtained which were grouped in two matrices: the air test matrix, respectively the liquid lead test matrix. The two matrices of the results contain the following quantities: Yield stress, $\sigma_{0.2}$; Ultimate tensile strength, σ_r; Ramberg - Osgood relationship α parameter; The parameter m , which is the inverse of the hardening coefficient, *n*.

Examination of the tensile curves mechanical stress-strain of the samples tested in air and liquid lead resulted in the following observations:

- For the temperature of 350ºC, although the breaking strength decreases in lead to air, in terms of elongation at fracture, the difference is only a few percent.
- For temperatures of 375ºC and 400ºC there is a decrease in ductility, by reducing the total deformation at fracture in the liquid lead environment compared to the tests performed in the air environment. This means that the presence of LME cannot be neglected at these deformation rates in traction. At the same time, there is a decrease in ultimate tensile strength for liquid lead testing, which can also be attributed to the LME effect on 316L samples, tested in SSRT traction.

Following **the metallographic examinations** of the samples tested in the air and the liquid lead, the following can be concluded:

- At 350ºC, the behaviour of the samples, respectively of the cracking fronts, is not significantly different in lead from the air.
- For the temperatures of 375ºC and 400ºC a significant change of the character of the cracking front was observed, namely, the appearance of the features that characterize a fragile rupture. It can be assumed that this is due to the initiation of the LME mechanism during testing, especially at low strain rates (SSRT).

Following **the SEM examination** of the samples tested in air and liquid lead, the following statements can be made:

- For the samples tested in the air at a temperature of 350ºC and for the lowest deformation rate (SSRT type), the formation of microcavities (gaps) can be noticed, and some of them are placed inside larger cavities of cup-cone type. This way of breaking is typical of the ductile breaking of metals. For tests performed in lead, at the same temperature the SEM analysis of the fracture surfaces shows the same morphology of the microcavities, similar to the tests performed in the air, namely, large cavities whose walls contain microcavities (holes). Thus, it can be noted that the presence of LME due to lead is not evidenced by SEM analyzes at this temperature.
- For samples tested in the air at 375ºC a typical SEM surface, for SSRT type speed, observed at x1000 magnification, the morphology of the microcavities is similar to that observed at 350°C. This maintains the ductile character of the specific fracture of metals. For the tensile tests carried out in the liquid lead at this

temperature and deformation rate, the mixed ductile-brittle character appears. In this case, part of the fracture surface has microcavities, being bordered by a micro-cleavage-like area, which confirms the presence of the LME mechanism caused by liquid lead during the tensile test.

- For tensile tests performed in the air at a temperature of 400ºC, for a typical SEM surface, for SSRT type speed, at x1000 magnification, the morphology of the microcavities is characterized by an increase in their dimensions as well as by the multiplication of larger cavities, explained by the increased ductility of 316L steel with increasing temperature. For tensile tests performed in the liquid lead at this temperature and low deformation rate, the fracture surface mainly shows cleavage areas confirming the fragility of the LME produced by liquid lead during the tensile test.

NEW: Analysis - Modeling

The novelty and originality aspects of the results obtained in the analysis and modelling performed in this report of the doctoral study are described below.

- A first novelty is the performance of experimental tensile tests on samples of 316L austenitic stainless steel, in the liquid lead and the air, to characterize the influence of liquid lead embrittlement on the thermomechanical behaviour in the temperature range 350°C - 400°C, the specific operating mode of the ALFRED demonstrator.
- Another novel aspect is the method of obtaining the coefficients α and m the constitutive equation defining the Ramberg - Osgood, which characterizes the behaviour of the elastic-plastic ductile material under the application of uniaxial tension.
- An original feature of the doctoral study is the obtaining of an analytical model with practical utility, by processing the experimental results. This is done by using the method of the artificial neural network type "Multilayer Feedforward Neural Network"(abbreviated MFNN), in the MATLAB programming environment. This modern working method was proposed because the preliminary analysis of the experimental data showed a considerable spread for the parameter values: yield stress, ultimate tensile strength, calculated values of the parameters α and *m*. Thus, modelling by the method of MFNN leads to fairly accurate prediction functions for α and m. At the same time, it should be noted that the explicit MFNN type functions obtained have as input several important modelling parameters: ***temperature, strain rate, yield stress, ultimate tensile strength***. This model also admits its further improvement with the accumulation of new experimental data as well as the knowledge of new parameters of influence (oxygen concentration in lead, etc.). Such modelling, in which to enter several input parameters is very difficult to achieve by the usual fitting methods with which the statistical packages from various programs are provided.
- Another novelty is the application of fracture mechanics described in the report, which uses the Ramberg - Osgood relationship with the coefficients rendered by explicit MFNN functions, to simulate the behaviour of breaking mechanics under LME conditions, in the liquid lead at 400°C, as well as in the air, for 316L steel. For this, the micro-mechanical model of the Gurson-Tvergaard-Needleman ductile fracture was used. The model was implemented in the FEACrack fracture mechanics software, the stress and strain analysis being performed by the finite element method. The obtained results are following the results of the experimental tests performed in the doctoral study but also with the similar ones mentioned in the literature.

The literature mentions the different mechanical behaviour in the liquid lead environment compared to the air environment of 316L steel, for the specified temperature range, being included in the statistical field of experimental errors. Instead, as a corollary of the novelty and originality aspects mentioned above, the arguments presented in the thesis suggest that these differences exist, are real and can be highlighted analytically, as was done in this doctoral study.

APPLICATION: Structural Integrity - Perspectives

The exemplification of the possibilities of practical use of the results of the doctoral study was achieved by implementing a model based on the Gurson-Tvergaard-Needleman (GTN) approach to evaluate the initiation and propagation of cracks under LME conditions on 316L austenitic stainless steel. The analysis was performed with the finite element method, through the fracture mechanics software, FEACrack, highlights the cracking due to LME, in typical fracture mechanics tests, Compact-Tension (CT), and the results are consistent with those in the literature.

The results of the doctoral study will be used practically in the structural integrity analysis activities, performed with the help of various calculation codes, which will be used in the evaluations of the ALFRED demonstrator, which will be built at RATEN ICN.

Selective Bibliography:

[1] M. Frogheri, A. Alemberti and L. Mansani, "*THE ADVANCED LEAD FAST REACTOR EUROPEAN DEMONSTRATOR (ALFRED)*", The 15th International Topical Meeting on Nuclear Reactor Thermal - Hydraulics, NURETH-15 Pisa, Italy, May 12-17, 2013.
[2] *ALFRED Project Lead Cooled Fast Reactor Demonstrator* - General Presentation- Romanian Perspective.
[3] Gorse-Pomonti, D. and V. Russier (2007), "*Liquid Metals for Nuclear Applications*", Journal of Non-Crystalline Solids, 353, pp. 3600-3614.
[4] Lyutyi EM (1987) "*Problems of high-temperature liquid metal corrosion of refractory metals and alloys"*, Mater Sci 24 (5): 441–445.
[5] PJL Fernandes, RE Clegg, and DRH Jones: *Eng. Fail. Anal.*, 1994, **1,** 51-63;
[6] ASTM G 129-00, "*Standard Practice for Slow Strain Rate Testing to Evaluate the Susceptibility of Metallic Materials to Environmentally Assisted Cracking*", 2000.
[7] ASTM E8 / E8M, "*Test Methods for Tension Testing of Metallic Materials*", 2009.
[8] T. L. Anderson, *Fracture Mechanics, Fundamentals and Applications*, CRC Press, 1995.
[9] FEACrack V.2.7.000, "Structural *Reliability Technology* ", Boulder USA.
[10] Metallography: An Introduction, "*Metallography and Microstructures"*, Vol. 9, ASM Handbook, ASM International, 2004, pp. 3–20.
[11] Nuclear Science, "*Handbook on Lead-bismuth Eutectic Alloy and Lead Properties, Materials Compatibility, Thermal-hydraulics and Technologies*", 2015, No. 7268.
[12] Z. Hamouche-Hadjem et al, "*Susceptibility to LME of 316L and T91 steels by LBE: Effect of strain rate*", Journal of Nuclear Materials 376 (2008), 317 - 321.
[13] Ingrid Serre, Jean-Bernard Vogt, " *Mechanical properties of a 316L / T91 weld joint tested in lead-bismuth liquid* ", Material and Design 30 (2009), 3776 - 3783.
[14] Dieter, George, JR., *Mechanical Metallurgy*, McGraw-HILL BOOK Company, 1961.
[15] Ramberg, W., Osgood, RW, " *Description of stress-strain curves by three parameters* ", National Advisory Committee of Aeronautics, Technical Note 902, National Bureau of Standards, Washington, DC, USA, 1943.
[16] Matlab R2017b, The MathWorks, Inc.USA.
[17] *FEACrack, "3D Finite Element Software for Cracks", User's Manual, QuestIntegrity, USA*
[18] Simon Haykin, Neural Networks, A comprehensive foundation, Pearson Education, 1999.
[19] Kiran, R., Khandelwal, K., "Gurson model parameters for ductile fracture simulation in ASTM A992 steels", Wiley Publishing Ltd, Fatigue & Fracture of Engineering Materials & Structures 00, 1-13, 2013.
[20] Gurson, AL, „Continuum theory of ductile rupture by void nucleation and growth. I. Yield criteria and flow rules for porous ductile media", Transaction of ASME Series H, Journal Engineering Materials Technology, 99, 2, 1977.
[21] ASTM E646-07, "Standard Test Method for Tensile strain-hardening Exponents (n -Values) of Metallic Sheet Materials", 2007.
[22] ASTM E1820-11, "*Standard Test Method for Measurement of Fracture Toughness"*, 2011.
[23] OECD Nuclear Energy Agency (NEA), "Handbook on Lead-bismuth Eutectic Alloy and Lead Properties, Materials Compatibility, Thermal-hydraulics and Technologies", No. 7268, 2015.
[24] Lorenzo Stefanini, "*Influence of Lead-Bismuth Eutectic Environment on the mechanical properties of the AISI 316L stainless steel*", Pisa, 20 July 2015.